How Crashes Develop: Intradaily Volatility and Crash Evolution

David S. Bates*

January 15, 2018

Abstract

This paper explores whether affine models with volatility jumps estimated on intradaily S&P 500 futures data over 1983 to 2008 can capture major daily outliers such as the 1987 stock market crash. Intradaily jumps in futures prices are typically small; self-exciting but short-lived volatility spikes capture intradaily and daily returns better. Multifactor models of the evolution of diffusive variance and jump intensities improve fits substantially, including out-of-sample over 2009 to 2016. The models capture reasonably well the conditional distributions of daily returns and of realized variance outliers, but underpredict realized variance inliers. I also examine option pricing implications.

Forthcoming, *Journal of Finance*

*David Bates is with the University of Iowa and the National Bureau of Economic Research. I am grateful for comments on earlier versions of the paper from seminar participants at Iowa, Northwestern, Houston, Lugano, and the Collegio Carlo Alberto, and from conference participants at the 2012 IFSID Conference on Structured Products and Derivatives, McGill University's 2014 Risk Management Conference, the 2016 FMA/CBOE Conference on Volatility and Derivatives, and the 2017 annual conferences of the Midwest Finance Association and Society for Financial Econometrics. I have read the *Journal of Finance*'s disclosure policy and have no conflicts of interest to disclose.

Electronic copy available at: https://ssrn.com/abstract=2732875

What is a crash? In the jump-diffusion model of Merton (1976), a crash is a rare event – a single adverse draw from a Poisson counter, with a vanishingly small probability of multiple adverse draws within a single day. While this model may be successful at capturing outliers in daily returns, it does not appear to capture the intradaily evolution of major market downturns. The 28% drop in the December 1987 S&P 500 futures price on Monday, October 19, 1987 (23% drop in the S&P index) from the preceding Friday's closing level did not occur within five minutes, for instance; it took all day to achieve the full decline. Indeed, papers such as Tauchen and Zhou (2011) that use the bipower variation approach of Barndorff-Nielsen and Shephard (2004, 2006) to decompose realized variance into diffusive and jump components suggest there were no jumps at all on October 19! Instead, it was a draw of roughly two standard deviations from a day that happened to have an unusually high intradaily realized volatility of 12%.

While the increasing availability of high-frequency data has generated some exploration of intradaily volatility evolution, including in stock markets, there has been little direct estimation of dynamic models with stochastic volatility and jumps using intradaily data. Papers such as Andersen and Bollerslev (1997) focus on volatility dynamics; in particular, on reconciling GARCH-based volatility evolution estimates from daily versus intradaily data. As described in Andersen (2004), the recognition that realized variance effectively summarizes intradaily volatility information *and* sidesteps the issues of fitting pronounced diurnal volatility patterns and announcement effects shifted the focus of most intradaily research to realized variance. Whether jumps are important has been assessed indirectly in this literature, using either the bipower variation approach of Barndorff-Nielsen and Shephard (2004, 2006) or the threshold approach of Mancini (2009) to assess intradaily jump contributions to realized variance. Those approaches maintain the Merton (1976) presumption that jumps are rare.

This indirect evidence and more direct parametric estimates by Stroud and Johannes (2014) on intradaily data indicate a fundamental mismatch between jump magnitudes from intradaily versus from daily stock market data, let alone those inferred from option prices. Stroud and Johannes estimate 0.2% to 0.4% for the standard deviation of unexpected jumps in 5-minute

Electronic copy available at: https://ssrn.com/abstract=2732875

returns, and similar magnitudes for predictable announcement effects. The jump magnitudes estimated by Bates (2012, Table 6) on daily data over 1926 to 2006 using a double exponential jump distribution are an order of magnitude higher: -2.1% on average for negative jumps, and +1.6% for positive jumps. The double exponential jump parameters inferred from stock index options by Andersen, Fusari, and Todorov (2015; henceforth **AFT**) are even larger: -3.9% on average for risk-neutral negative jumps, +2.7% for risk-neutral positive jumps. One must, of course, be wary of parameter inferences from option prices; standard equity and volatility risk premia imply the frequency and magnitude of negative jumps are greater under the risk-neutral than under the actual distribution. However, those effects are reversed for positive jumps, implying one should observe even larger (and more frequent) positive jumps on average than the +2.7% estimate in AFT (2015).

The objective of this paper is to bridge the gap between intradaily and daily evidence on stock market returns, and to explore continuous-time affine models that might be compatible with both. The key feature of the models is "self-exciting" synchronous and correlated co-jumps in intradaily stock returns and volatility; essentially a stochastic intensity and multifactor generalization of the Duffie, Pan and Singleton (2000) volatility jump model. Every small intradaily jump substantially increases the probability of more intradaily jumps in volatility and in returns; and these can accumulate into the major outliers in daily returns that we occasionally observe. The model is estimated on intradaily and overnight S&P 500 futures returns over 1983 to 2008 via the Bates (2006, 2012) Approximate Maximum Likelihood (AML) filtration methodology, taking into account special features of intradaily futures data. Estimates are then tested for compatibility with daily returns – including movements exceeding 10% in magnitude in 1987 and 2008. The 2009 to 2016 period is used for various out-of-sample tests of the model.

The central two mechanisms in the model are volatility feedback (via jumps) and leverage: a tendency of conditional volatility to become more volatile at higher levels that is combined with negative correlations between price and volatility shocks. These have been proposed and estimated on daily data, using a variety of models and estimation methodologies. The diffusive

affine stochastic volatility model of Heston (1993) has both, and has been estimated on daily stock market data by various authors surveyed in Bates (2006, Table 7). The nonaffine diffusive log variance models in Chernov et al (2003) have substantial volatility feedback; the CEV diffusive variance model in Jones (2003) has even more. Models with jumps typically have leverage but not volatility feedback through jump channels: e.g., the price/volatility co-jump model of Eraker, Johannes and Polson (2003) estimated by MCMC on daily data, and the co-jump model of Stroud and Johannes (2014) that is estimated on intradaily data. Neither of these papers has self-exciting jumps. Calvet and Fisher (2008) propose a tightly parameterized Markov Chain model for daily log variance evolution that also lacks volatility feedback. Aït-Sahalia, Cacho-Diaz and Laeven (2015) and Fulop, Li and Wu (2015) have affine models with stochastic volatility and self-exciting volatility jumps, which they estimate on daily stock market data. AFT (2015) have a model of self-exciting price/volatility co-jumps similar to the one used here, which they estimate primarily from options data.

The nonparametric literature does of course make extensive use of intradaily returns, typically at a 5-minute horizon. That literature has primarily focused on decomposing intradaily realized variance into diffusive and jump components, and on developing tests of the null hypothesis of no jumps or co-jumps.[1] These can also be done in the affine parametric framework used here. Any affine latent characteristic can be estimated from observed data by Bayesian filtration methods discussed in this paper: the number and size of stock market jumps, quadratic variation and its diffusive variance and squared jump components, and even the magnitude of volatility jumps. Nested models without volatility jumps can be tested via standard likelihood ratio tests.

However, the key difference of this paper relative to the realized variance literature is its focus on the intradaily *dynamics* of diffusive variance and jump intensities. Nonparametric

[1] See Jacod and Todorov (2010) for statistical tests of price/volatility co-jump models, and Bandi and Renò (2016) for nonparametric estimates of co-jump models on S&P futures returns over 1982 to 2009. The latter includes a model in which the mean and volatility of price jumps are affected by the level of conditional volatility – another form of volatility feedback.

estimates have an aliasing problem: if integrated diffusive variances are estimated each day from intradaily data by bipower variation or threshold techniques, the approach can at best describe the daily dynamics of the series. This paper by contrast estimates dynamic models on intradaily data to see whether volatility feedback in the form of self-exciting volatility/price co-jumps is present at intradaily frequencies. The sign and magnitude of every 15-minute return contains important information for the probability of future price/volatility co-jumps over the next 15 minutes. That includes not just the large price movements that nonparametric methods can readily identify as jumps, but also the more ambiguous movements of three to five diffusive standard deviations that *might* be jumps.[2] The explicit parametric models in this paper provide the structure for extracting that information, via a recursive filtration procedure that updates assessments every 15 minutes of underlying diffusive volatility and jump intensity state variables.

I explore four issues. First is the specification issue of identifying the appropriate time series model, using an extensive history over 1983 to 2008 of intradaily and overnight S&P 500 futures returns that includes extreme stock market movements in October 1987 and in the fall of 2008. I build up the models progressively, starting with a model with price jumps but not volatility jumps, adding volatility co-jumps, and adding richer dynamics for the evolution of diffusive volatility and jump intensities. I also look at models without the self-exciting feature. I find that multifactor models with self-exciting but short-lived volatility spikes substantially improve model fits both in sample and out of sample.

Second is the issue of time aggregation: do various proposed affine models estimated using 15-minute returns actually capture the statistical properties of daily returns – including major daily outliers in 1987 and 2008? Affine models are especially suited for exploring this issue, because affine models time-aggregate. An affine model for intradaily returns implies an affine model for daily returns that can be used for standard QQ diagnostics of conditional distributions.

[2] See Bates (2006, pp. 942-3) or Aït-Sahalia and Jacod (2014, pp. 118-9) for discussions of this issue.

Third is how well the models capture the statistical properties of daily realized variances. Insofar as realized variance is approximately quadratic variation, which is affine, QQ diagnostics similar to those used for daily returns can be used for realized variances. (In practice, simulation-based bias corrections prove necessary.) The paper also looks at the models' ability to forecast realized variances at 1- to 21-day horizons, as a precursor to the final model criterion: how well the models fit short-maturity option prices.

Section I of the paper describes the intradaily and overnight data, the multifactor models and estimation methodology, and how well the models fit. Section II contains additional diagnostics using intradaily realized variance, while Section III explores option pricing fits. Section IV concludes. Overall, the multifactor affine models with volatility spikes do a reasonably good job of matching the properties of intradaily and daily S&P 500 futures returns, especially as more factors are added. Furthermore, the most general three-factor model captures the occasionally extreme observations of realized variance reasonably well; and those are when extreme daily stock market returns occur. The models underpredict the frequency of small realized variance observations, however, indicating that some specification error remains. Similarly, the more general models do fit the overall level of options' implicit volatilities progressively better. However, all models have difficulty matching the slope of the volatility smirk at maturities greater than the shortest one-day horizon considered.

I. Data and models

A. Data

S&P 500 futures began trading at the Chicago Mercantile Exchange (CME) on April 21, 1982, using the open-outcry pit trading prevailing at the CME at that time for all futures contracts. Initial trading hours were 9 AM to 3:15 PM Central Standard Time, with CME pit trading typically extending 15 minutes beyond trading at the New York Stock Exchange (NYSE).[3] On September 30, 1985, the NYSE and CME shifted the opening time by a half-hour, to 8:30 AM CST. Starting

[3] The CME and NYSE closed at the same time over October 23 through November 6, 1987, in the aftermath of the 1987 stock market crash.

in December 1990, both the NYSE and CME instituted fewer trading hours on trading days adjacent to Christmas, the Fourth of July, and Thanksgiving.

In 1992, the CME introduced after-hours electronic trading through its Globex trading platform. In 1997, the CME introduced "E-mini" (ES) S&P 500 futures contracts, which are 1/5th the size of regular S&P 500 (SP) futures contracts and trade exclusively on Globex, including during the day. Activity switched increasingly to electronic trading via Globex, which accounted for 84% of CME group volume by 2011.[4]

The CME provides data in two formats: "End-of-Day" daily summaries and "Time and Sales" data. The former contains open, high, low, close, and settlement prices, as well as volume and open interest, while the latter contains the time and price of every daily transaction in which the price changed from the previous transaction. Bid and ask prices are also recorded when the bid price is above or the ask price is below the price of the previous transaction. No information is provided for the pit-traded contract regarding the volume of transactions at a particular price, but is provided for the E-minis. I acquired both sets of data for the original full-sized S&P 500 futures SP contract for January 3, 1983 through December 31, 2013, and for the entire history of the E-mini ES contract from September 7, 1997 through June 30, 2016. I discarded the bid and ask data, and also transactions that were subsequently cancelled. The SP data over 1983 to 2008 are used for parameter estimation, while E-mini data over 2009 to 2016 are used for out-of-sample testing.[5]

S&P 500 futures contracts typically mature on the third Friday of March, June, September and December – except for March 2008 contracts, which matured a day earlier because of Good

[4] CME Group, "Twenty Years of CME Globex," June 21, 2012. (http://www.cmegroup.com/education/files/globex-retrospective-2012-06-12.pdf).

[5] Comparison of the end-of-period times of SP and ES trades indicates little divergence over 1998 to 2008 (12.5 versus 2.5 seconds on average to the end of each 15-minute period), but increasing divergence thereafter. The SP average time gap rose from 25 seconds in 2009 to 135 seconds in 2013, while 15-minute intervals without transactions occurred increasingly frequently: 5 in 2011, 37 in 2012, and 166 in 2013. The ES time gap, by contrast, averaged about 1.4 seconds over 2009 to 2013. Absolute divergences in end-of-period SP and ES log futures prices were typically only 2 to 3 basis points throughout 1998 to 2013, but were occasionally larger during volatile days or on days adjacent to holidays.

Friday. Of the available maturities, I select the shortest maturity with nine or more days until the third Friday, that being the most actively traded contract according to the "End of Day" volume data. For instance, I used data for March 1983 futures maturing on March 18, 1983 up to the close of trading on Wednesday, March 9. Prices of June 1983 contracts are then used for computing overnight futures returns from Wednesday to Thursday, and for intradaily and overnight returns from Thursday, March 10 to the close of trading on Wednesday, June 8.

I construct intradaily 15-minute log-differenced futures prices broadly along the lines of the 5-minute futures returns in Chan, Chan, and Karolyi (1991) and Andersen and Bollerslev (1997), by taking the last observed future price in every interval. 15-minute returns were used instead of 5-minute primarily to triple optimization speed on this large data set, but also to span some short-duration price limit constraints on futures returns over 1989 to 2002 that are discussed below. For after-hours trading, I extend the time window by one minute, typically up through 3:16 PM CST, because trades were often recorded shortly after trading had officially ended. Overnight futures returns are constructed as the difference between the log of the futures price at the end of the first 15-minute trading session (typically 8:30 to 8:45 AM CST) and the log of the futures price of comparable maturity at the end of the preceding day. This approach allows some time for the incorporation of overnight news into the futures price, during the especially volatile initial fifteen minutes of trading. Furthermore, skipping the first 15 minutes when computing overnight returns spans possible constraints on opening futures prices from the price limit system instituted by the CME in 1989. The final SP data set has 6,557 overnight returns and 168,297 intradaily returns, from December 31, 1982's closing price through December 31, 2008. The E-mini data over 2009 to 2016 has 1,885 overnight returns and 48,825 intradaily returns.

The CME's price limit system was created in response to the stock market crash of October 19, 1987, and paralleled the NYSE's "circuit breaker" system. The CME's price limits typically involved four prespecified constraints: a relatively tight initial band relative to the previous day's short-maturity S&P 500 futures settlement price that temporarily constrained both upward and downward moves at the open, and three progressively lower price limits (Levels 1 through 3) that

temporarily constrained downward moves during the day. Hitting a price limit triggers a specific time interval during which the price limit remains in effect, followed by a two-minute trading halt if the price limit is binding ("locked limit"), followed by the resumption of trading with a new and lower price limit in effect. For instance, price change constraints over 1989 to 1996 were 5, 12, 20, and 30 points, respectively, over which time the S&P 500 index rose from 300 to 700. The 5-point opening limit lasted only until 8:40, with a trading halt from 8:40 to 8:42 if binding. A 12-point downward move triggered an interval lasting 30 minutes or until 2:30 PM CST, during which time futures contracts could be traded at or above the limit but not below. If the price limit was binding at the end of the interval, a two-minute trading halt was declared, followed by the resumption of trading with the 20-point lower limit in place. Hitting the 20-point downward limit started another interval of 30 minutes or until 2:30, followed by a trading halt (if still binding) and the 30-point limit taking effect for the remainder of the day. Separate rules apply if the futures price was locked limit at the close of the preceding day.

Limits on the opening price change were removed on October 15, 1997, as part of a revision in the circuit breaker system. The levels of permissible downward price changes changed over time, partly because of the rise and fall in the level of the S&P 500. In addition, the price constraints were significantly widened on May 13, 2001 to roughly 5%, 10%, and 15% of the end-of-quarter S&P 500 level, with roughly 20% being the maximal permissible daily price movement. These limits were relaxed further in January 2008 to 10%, 20% and 30%, respectively, to be consistent with the Dow Jones based percentages used on the NYSE. (A 5% price limit remained on after-hours trading on Globex.) These revisions in 2001 and 2008 considerably reduced the frequency of trading halts, with an apparent absence of such halts in intradaily data over 2003 to 2008.[6] Even the 10.4% intradaily drop in the December 2008 futures price on October 15, 2008, to 898.5 from October 14's settlement price of 1002.3, did not exceed the 120-point limit that the CME had set on September 30, 2008 as the 10% limit for the fourth quarter of 2008.

[6]John Nyhoff at the CME kindly provided me with a list of dates and times when the S&P 500 futures price limits were hit during regular trading hours. Stroud and Johannes (2014) note that the GLOBEX-traded E-mini contract hit its overnight limit on October 24, 2008.

The corresponding time intervals triggered by hitting a price limit were also shortened to roughly 15 minutes in 1996, and to roughly 10 minutes in 1997. However, longer halts could ensue contingent upon trading halts at the NYSE. The major such incident was the tripping of all three levels of NYSE circuit breakers on October 27, 1997.

Trading at the CME also occasionally halted because of exogenous events in New York or Chicago. On December 27, 1990, for instance, the explosion of a Con Edison transformer in New York delayed the open of the NYSE and CME. On April 13, 1992, the accidental flooding of utility tunnels in Chicago shut down the CME, but not the NYSE.[7] Both the NYSE and CME closed following the attacks on September 11, 2001, and did not reopen until September 17.

Price limits can artificially constrain observed futures returns. Consequently, I extended the time interval whenever a price limit was hit until that limit had expired and was no longer potentially binding on the futures price. Similarly, I extended time intervals whenever trading was suspended until trading had resumed, and computed returns over the expanded interval. For instance, the CME suspended trading at 11:15 AM CST on October 20, 1987, the day after the 1987 stock market crash;[8] and the December 1987 futures price rebounded when the trading resumed at 12:05 PM. I combined returns over 11:15 AM to 12:15 PM into a single one-hour interval, with an associated log-differenced futures price of 13.76%.[9] There were 103 instances over 1983 to 2008 of expanded time intervals, out of 174,859 total observations. The E-mini data had 3 instances over 2009 to 2016 of expanded time intervals, out of 50,710 total observations.

B. Models

Affine models allow considerable flexibility in how diffusive spot variance and jump intensities evolve, and the precise interactions between shocks to futures returns and to the

[7] A list of market closings at the NYSE is available at http://www.nyse.com/pdfs/closings.pdf. Additional CME trading suspensions were identified by searching the data for periods without reported trades, and matching them against news reports.
[8] See Carlson (2006, p.11).
[9] Andersen and Bollerslev (1997) follow Chan, Chan and Karolyi (1991) in omitting data over October 15 through November 13, 1987. They also linearly interpolate prices when data are missing, yielding roughly identical successive 5-minute returns.

underlying state variables. I model the continuous-time process for the log futures price $f_t = \ln F_t$ underlying observed intradaily and overnight S&P 500 futures returns as a potentially multifactor affine jump-diffusion of the form

$$\begin{aligned} df_t &= \mu_0 dt + \sum_{i=1}^{I}\left[(\mu_i - ½)V_{it}dt + \sqrt{V_{it}}dW_{it}\right] + \sum_{j=1-K}^{J}\left(\gamma_j dN_{jt} - \lambda_{jt}\bar{k}_j dt\right) \\ dV_{1t} &= (\alpha - \beta_1 V_{1t})dt + \sigma\sqrt{V_{1t}}dW_{Vt} + \gamma_{V1}dN_{1t} \\ dV_{it} &= -\beta_i V_{it}dt + \gamma_{Vi}dN_{it} \text{ for } i > 1, \end{aligned} \tag{1}$$

where W_{1t} and W_{Vt} are Wiener processes with correlation ρ, W_{it} for $i > 1$ are additional orthogonal Wiener processes, the N_{jt}'s are Poisson counters with stochastic intensity λ_{jt} that depend linearly upon the state variables $\boldsymbol{V}_t = (V_{1t}, \ldots, V_{It})'$, and $\bar{k}_j = E(e^{\gamma_j}) - 1$ is the *j*th expected percentage jump size in futures. Furthermore, the state variables are divided into a core jump-diffusive variance state variable V_{1t}, and additional pure-jump state variables V_{it} that capture transient variance shocks.

A key empirical issue is how many state variables are necessary to adequately summarize the diffusive and jump risks underlying futures returns. Potential specifications are categorized as SVJ(*I,J,K*) models, where *I* is the number of underlying state variables, *J* is the number of synchronous jump processes for futures prices and variance state variables, and $K \leq 1$ is the number of jump processes for futures prices only.

Another important issue is the precise joint distribution of the (γ_j, γ_{Vj}) co-jumps. Affine models require $\gamma_{Vj} \geq 0$ to preclude negative variances, but otherwise place no restrictions on this joint distribution. I use the Duffie, Pan and Singleton (2000; henceforth **DPS**) specification:

$$\gamma_j = \rho_j \gamma_{Vj} + \gamma_{fj} \tag{2}$$

where $\gamma_{Vj} \sim Exp(\bar{\gamma}_{Vj})$ is the exponentially distributed jump in spot variance V_{jt} conditional upon $dN_{jt} = 1$, $\gamma_{fj} \sim N(\bar{\gamma}_{fj}, \delta_{fj}^2)$ is an independent Gaussian shock, and ρ_j captures the degree to which synchronous jumps in futures prices and variance covary. The Poisson counter N_{0t} identifies additional futures price jumps (with a V_{1t}-sensitive jump intensity) that are unaccompanied by volatility jumps – an extension that substantially improves overall fits. Volatility jumps that are unaccompanied by price jumps are also possible if $(\rho_j, \bar{\gamma}_{fj}, \delta_{fj}^2) = \mathbf{0}$.[10]

The final issue is the specification of jump intensities. Whereas DPS is a constant intensity model, self-exciting jumps are plausibly a major explanation for the intradaily development of major daily outliers.[11] For tractability, I use jump intensities of the general form

$$\lambda_{jt} = \begin{cases} \lambda_{j0} + \lambda_{j1} V_{1t^*} & \text{for } j \leq 1 \\ \lambda_{j0} + \lambda_{j1} V_{1t^*} + \lambda_{jj} V_{jt^*} & \text{for } j > 1, \end{cases} \tag{3}$$

with specific parameter restrictions discussed further below. The jump intensities λ_{jt} for each Poisson counter N_{jt} are assumed constant within each intradaily or overnight period, reset at the end of every period, and depend upon the spot variance levels $\boldsymbol{V}_{t^*}$ prevailing at the start of the period. This allows jumps to be self-exciting across periods, while retaining the analytic tractability of the DPS model. The recursive structure in (3) for $j > 1$ allows the initiation of additional self-exciting volatility components V_{jt} to depend upon the level of core volatility V_{1t}.

The multifactor specification for $\boldsymbol{V}_t$ from equations (1) to (3) allows considerable flexibility in how underlying diffusive variances and jump intensities can evolve. For instance, the multifactor specification (1) nests a univariate model with variance jumps drawn from a mixture of exponentials, when the rates of mean reversion β_i are identical and jump intensities are similarly restricted. More generally, multivariate models allow the distributions of jumps in stock

[10] Andersen, Fusari and Todorov (2015) propose an interesting but less tractable model in which the futures jump γ_j has a double exponential distribution, and variance jumps are the weighted average of the negative price jump component squared and an additional independent squared exponential shock.
[11] See, e.g., Fulop, Li and Yu (2015) for estimates of such a model from daily stock index returns.

market returns and in total diffusive spot variance to vary as the components of $\boldsymbol{V}_t$ change. Those components can have different degrees of persistence, and different correlations with the contemporaneous stock market returns from which they are estimated. Because the V_{it}'s are independent *AR*(1) processes, total diffusive variance and jump intensities follow $ARMA(I, I-1)$ processes.

The model does not explicitly consider scheduled announcement effects, which Prokopczuk and Semen (2014) estimate at 25% of observed jumps in E-mini futures prices during regular business hours over 2008 to 2014.[12] Major macroeconomic announcements are treated as randomly timed jumps, with the schedule unexploited in the above specification (3) of jump intensities. Furthermore, the estimates below implicitly assume that such announcements have the same self-exciting dynamic implications of other jumps. Stroud and Johannes (2014) provide a detailed look at the volatility impact of various major scheduled announcements, most of which are deliberately scheduled outside of regular business hours.

Affine models such as equations (1) to (3) imply the joint cumulant generating function of returns $y_{t+1} = f_{t+1} - f_t$ and future spot variances $\boldsymbol{V}_{t+1}$ given current $\boldsymbol{V}_t$ is affine in $\boldsymbol{V}_t$,

$$\begin{aligned} CGF(\Phi, \boldsymbol{\psi} | V_t, \tau_t) &= \ln E\left[\mathrm{e}^{\Phi y_{t+1} + \boldsymbol{\psi}' \boldsymbol{V}_{t+1}} \mid \boldsymbol{V}_t\right] \\ &= C(\tau_t; \Phi, \boldsymbol{\psi}) + \boldsymbol{D}(\tau_t; \Phi, \boldsymbol{\psi})' \boldsymbol{V}_t. \end{aligned} \tag{4}$$

where τ_t is the time horizon. The precise functional forms of $C(\cdot)$ and $\boldsymbol{D}(\cdot)$ for the various SVJ(*I*,*J*,*K*) models are in Appendix A. By iterated expectations, the joint conditional cumulant generating function conditional upon observing past data $\boldsymbol{Y}_t = \{y_1, \ldots, y_t\}$ is then of the form

[12] Prokopczuk and Semen use a Lee and Mykland (2008) nonparametric jump estimation procedure at a 5-minute frequency, with adjustments for diurnal effects. They find that another 25% of jumps are attributable to major but unscheduled news, with the remaining 50% unassociated with any observable news. They also find that unscheduled jumps have three times the overall variance contribution of scheduled jumps.

$$\begin{aligned} CGF(\Phi, \boldsymbol{\psi} | \boldsymbol{Y}_t, \tau) &= \ln E\{\exp[\Phi y_{t+1} + \boldsymbol{\psi}' \boldsymbol{V}_{t+1}] \mid \boldsymbol{Y}_t\} \\ &= C(\tau_t; \Phi, \boldsymbol{\psi}) + g_{t|t}[\boldsymbol{D}(\tau_t; \Phi, \boldsymbol{\psi})] \end{aligned} \tag{5}$$

where $g_{t|t}(\boldsymbol{\psi}) \equiv \ln E\left[e^{\boldsymbol{\psi}' \boldsymbol{V}_t} \middle| \boldsymbol{Y}_t\right]$ is the cumulant generating function of $\boldsymbol{V}_t$ conditional upon data $\boldsymbol{Y}_t$. How to compute $g_{t|t}(\boldsymbol{\psi})$ recursively via Bayesian filtration is discussed further below.

C. Rounding models and filtration

Because SP S&P 500 futures had a price tick size of 0.05 through October 31, 1997, and 0.10 thereafter, observed intradaily futures returns are not drawn from a continuous distribution. Indeed, 5% of all intradaily 15-minute returns over 1983 to 2008 are exactly zero despite intervening intraperiod price changes,[13] while 42% are over a range of ±5 price ticks. The E-minis had a tick size of 0.25 throughout 1997 to 2016, and 42% of E-mini absolute price changes were 0 to 3 price ticks over 2009 to 2016. Consequently, the above continuous-time models are assumed to represent the underlying conditional distribution of futures returns; and those returns are rounded to the futures returns actually observed. The scaled probability of an observed log futures return $y_{t+1} = \ln(F_{t+1}/F_t)$ over a horizon of length τ_t is computed via Fourier inversion as the integrated conditional density of all realizations falling within ±½ price tick of the observed F_{t+1}:

$$\begin{aligned} P_{t+1} &= \frac{Prob\left[y_{t+1} \in \left(\underline{y}_{t+1}, \overline{y}_{t+1}\right) | \boldsymbol{Y}_t\right]}{\overline{y}_{t+1} - \underline{y}_{t+1}} \\ &= \frac{1}{2\pi} \int_{-\infty}^{\infty} e^{C(\tau_t; i\Phi, 0) + g_{t|t}[\boldsymbol{D}(\tau_t; i\Phi, 0)]} \frac{e^{-i\Phi \overline{y}_{t+1}} - e^{-i\Phi \underline{y}_{t+1}}}{i\Phi\left(\overline{y}_{t+1} - \underline{y}_{t+1}\right)} d\Phi \end{aligned} \tag{6}$$

$$\text{for } \underline{y}_{t+1} = \ln\left(\frac{F_{t+1} - \varepsilon/2}{F_t}\right), \overline{y}_{t+1} = \ln\left(\frac{F_{t+1} + \varepsilon/2}{F_t}\right), \text{and } \varepsilon = \text{one price tick.}$$

[13] There were on average 30 price changes per period for those intradaily periods with a futures return of zero.

Parameters are then estimated by maximizing the log likelihood function $\ln L = \sum_t \ln P_{t+1}$.[14] The computed probabilities are scaled by $\overline{y}_{t+1} - \underline{y}_{t+1}$ to make the results comparable in magnitude to log likelihood values based upon conditional probability densities.

The conditional moment generating function $G_{t|t}(\boldsymbol{\psi}) = \exp[g_{t|t}(\boldsymbol{\psi})]$ that summarizes what is known about $\boldsymbol{V}_t$ at time t can be updated recursively over time via a straightforward extension of the Approximate Maximum Likelihood (AML) methodology in Bates (2006, 2012):

$$G_{t+1|t+1}(\boldsymbol{\psi}) = \frac{1}{2\pi P_{t+1}} \int_{-\infty}^{\infty} e^{C(\tau_t; i\Phi, \boldsymbol{\psi}) + g_{t|t}[\boldsymbol{D}(\tau_t; i\Phi, \boldsymbol{\psi})]} \frac{e^{-i\Phi\overline{y}_{t+1}} - e^{-i\Phi\underline{y}_{t+1}}}{i\Phi\left(\overline{y}_{t+1} - \underline{y}_{t+1}\right)} \, d\Phi. \tag{7}$$

Derivatives of Equation (7) provide the noncentral posterior moments of $\boldsymbol{V}_{t+1}$ conditional upon adding the latest datum y_{t+1} to the data set:

$$E\left[V_{i,t+1}^n \middle| \boldsymbol{Y}_{t+1}\right] = \left. \frac{\partial^m G_{t+1|t+1}(\boldsymbol{\psi})}{\partial \psi_i^n} \right|_{\boldsymbol{\psi}=0}, \tag{8}$$

using analytical derivatives of the integrand in equation (7). These posterior moments are used to generate a gamma based moment matching approximation to $g_{t+1|t+1}(\boldsymbol{\psi})$ of the form

$$g_{t+1|t+1}(\boldsymbol{\psi}) = -\sum_{i=1}^{I} v_{i,t+1} \ln\left(1 - \kappa_{i,t+1}\psi_i\right). \tag{9}$$

where

$$\begin{aligned} E\left[V_{i,t+1} \middle| \boldsymbol{Y}_{t+1}\right] &\equiv \hat{V}_{i,t+1|t+1} = \kappa_{i,t+1} v_{i,t+1} \\ Var\left[V_{i,t+1} \middle| \boldsymbol{Y}_{t+1}\right] &\equiv P_{i,t+1|t+1} = \kappa_{i,t+1}^2 v_{i,t+1}. \end{aligned} \tag{10}$$

[14] This approach generalizes the Gaussian ordered-probit approach of Hausman, Lo, and MacKinlay (1992) to arbitrary underlying distributions (5). See Campbell, Lo, and MacKinlay (1997, Section 3.3.2) and Aït-Sahalia and Jacod (2014, Section 2.3.2) for overviews of rounding models.

The overall procedure is a version of robust Kalman filtration, and directly generates filtered estimates $\widehat{\boldsymbol{V}}_{t|t}$ of the latent state variables as a by-product.[15]

The realized variance literature has focused upon nonparametric estimation of the diffusive variance and jump components of intraperiod quadratic variation. In an affine model, these quantities are affine latent variables that can be directly estimated from observed futures returns, in the same fashion used above in equations (7) and (8) for estimating latent $\boldsymbol{V}_{t+1}$. I derive in Appendix A the relevant versions of $C(\cdot)$ and $D(\cdot)$ for computing $E[\Delta x_{t+1}|\boldsymbol{Y}_{t+1}]$ for various latent characteristics x_t of interest. This filtration procedure is similar to Lee and Mykland (2008) in using only past and current data to estimate diffusive variance and jumps for every period.[16]

D. Intradaily and overnight seasonals

The effective length of any time interval of course differs for overnight and intradaily 15-minute returns. In addition, there are intradaily variations in trading activity and volatility, as well as day of the week effects for intradaily and overnight effects. Finally, the actual length of a given trading day occasionally varies because of late openings or early closings – especially the half-day trading that began in December 1990 on specific days adjacent to Christmas, the Fourth of July, and Thanksgiving.

Wednesday is arbitrarily selected as the benchmark day, with Tuesday close to Wednesday close representing one full business day. The effective division between overnight returns (including the first 15 minutes of intradaily market trading) and intradaily returns (for the remainder of the day, typically until 3:16 PM CST) is estimated as variance proportions $(1 - f_{daily}, f_{daily})$, respectively. The daily time horizon $252\tau_{nm}$ on day n and time segment m is constructed as follows:

[15] Bates (2006) shows that AML parameter estimation efficiency is comparable to that of the Monte Carlo Markov Chain approach, for specific stochastic volatility processes with and without jumps. MCMC generates smoothed but not filtered estimates of latent state variables.

[16] Tauchen and Zhou (2011) and AFT (2015) by contrast use nonparametric smoothing procedures. All 5-minute returns in a given day are used to identify jumps at any time within that day.

$$252\tau_{nm} = \begin{cases} \left(1 - f_{daily}\right)\exp(\boldsymbol{\beta}_{ON}{}'\boldsymbol{d}_n^{ON}) \text{ overnight } (m = 0) \\ f_{daily}\dfrac{\exp[f(m, M_n)]}{\sum_{m=1}^{M_n}\exp[f(m, M_n)]}\exp(\boldsymbol{\beta}_{ID}{}'\boldsymbol{d}_n^{ID}) \text{ intradaily } (m > 0) \\ 5 - f_{daily}\exp\left(\beta_{Monday}\right) \text{ for Sept. 10 -17, 2001 (close to open)} \end{cases} \tag{11}$$

where $\boldsymbol{d}_n^{ON}$ are day of the week, holiday, and weekend dummies for overnight returns; $\boldsymbol{d}_n^{ID}$ are day-specific dummies for intradaily returns, including a half-day indicator for shortened trading days adjacent to holidays; and $M_n \leq 26$ is the number of 15-minute segments available on day *n* after the opening segment.

The function $f(m, M_n)$ follows Andersen and Bollerslev (1997) in using Gallant's (1981) flexible Fourier form approach to estimate the intradaily variance pattern:

$$\begin{aligned} f(m, M_n) = b_1\frac{m}{Avg_n(m)} + b_2\frac{m^2}{Avg_n(m^2)} + b_{ah}1(m = ah) \\ + \sum_{p=1}^{2}\left[c_p cos\left(2\pi p\frac{m}{M_n}\right) + d_p sin\left(2\pi p\frac{m}{M_n}\right)\right] \end{aligned} \tag{12}$$

where $Avg_n(m) = (M_n + 1)/2$, $Avg_n(m^2) = (M_n + 1)(M_n + 2)/6$, and $1(m = ah)$ indicates an after-hours trading segment at $m = M_n$.[17]

As discussed above, there were 103 occasions over 1989 to 2002 when intradaily futures returns were constrained by endogenous price limits or exogenous market closings. In such cases, I aggregate log futures returns over additional periods until the trading constraint or market closing is no longer in effect, and treat the yearly time interval associated with that aggregate log return as the sum of the spanned τ_{nm}'s. This approach is equivalent when filtering $\boldsymbol{V}_t$ to treating the subintervals of that full interval as missing observations.

[17] There were no after-hours sessions on October 23 through November 6, 1987.

Figure 1 shows the Vjump1b estimates of the intradaily and overnight variance patterns.[18] Overnight trading (including trading in the first 15 minutes of Wednesday morning) typically accounts for 18.8% of the return variance from Tuesday close to Wednesday close. Intradaily trading over the remainder of Wednesday accounts for the remaining 81.2%. These patterns are roughly comparable for other days of the week. As shown in Figure 1, there is a U-shaped weekly pattern to overnight return variance and an inverse U-shaped pattern to intradaily variance, with the sum of the two imparting a roughly flat but slightly increasing trend in business day variance across the week. Holidays during the week or as part of a holiday weekend substantially increase the variance of "overnight" returns that span those holidays. Intradaily trading on half-days adjacent to holidays have only 37.5% the variance of a regular intradaily trading interval.

Figure 1 about here

Figure 2 shows the intradaily pattern of effective time horizons for 15-minute returns over 8:45 AM through 3:16 PM for the longer trading days on September 30, 1985 through December 31, 2008, excluding the initial 8:30 to 8:45 interval. For comparison, period-specific average filtered quadratic variations and their diffusive variance, tiny jump and big jump components from the Vjump1b model are also plotted, as are period-specific realized variances observed over 1985 to 2008. The roughly U-shaped intradaily pattern in time horizons roughly reflects the intradaily pattern of realized variance. Average filtered quadratic variation is approximately but not exactly equal to average realized variance, with diffusive variance and tiny jump components responsible for 85% of the total intradaily quadratic variation. The realized variance and big jump outliers in the second 9 to 9:15 period appear attributable to large 3½ to 5% drops in the stock market on October 19, 20 and 22, 1987, rather than to regularly scheduled announcements at 9 AM CST.[19]

Figure 2 about here

The U-shaped pattern in time horizons and realized variances replicates Andersen and Bollerslev's (1997) Figure 6b, which was estimated on 5-minute S&P 500 futures returns using a GARCH model. Variance peaks in the afternoon at 2:15 to 2:30 PM CST and falls off thereafter,

[18] Because the results from other 1-factor models were almost identical, the Vjump1b time parameter estimates were also used in the multifactor Vjump2 and Vjump3 models, to speed up optimization.

[19] Andersen and Bollerslev (1998) find pronounced announcement effects evident in 5-minute currency returns at 9 to 9:05 AM CST.

especially in the after-hours 3 to 3:15 PM trading segment. Andersen and Bollerslev emphasize that it is critical to account for this periodic intradaily pattern, which if ignored would strongly affect estimates of variance mean reversion. Accounting for this intradaily periodicity is also important when estimating jump risk. Substantial distributional mixing is occurring, with opening and closing returns having roughly double the variance (40% higher volatility) of midday returns. Failing to account for this distributional mixing would exaggerate the conditional leptokurtosis of 15-minute returns, and boost the estimated magnitudes of intradaily jump risk.

E. Volatility and jump parameter estimates

Tables B.I to B.V in Appendix B contain estimates of the other jump-diffusion parameters that describe how diffusive spot variances $\boldsymbol{V}_t$ evolve, and the distributions of jumps. Five models are considered, all sequentially nested:

Model	**Variance processes**	**Jumps in log futures prices**
SVJ1	One-factor diffusive process for V_{1t}; no volatility jumps	Normally distributed jumps, with V_{1t}-dependent jump intensity.
Vjump1a	One-factor jump-diffusion	Jumps are correlated with V_{1t} jumps, and have a V_{1t}-dependent jump intensity.
Vjump1b	One-factor jump-diffusion	Two jumps: one uncorrelated with V_{1t} jumps, one correlated. Both have V_{1t}-dependent intensities.
Vjump2	Two-factor additive variance process. V_{1t} follows a jump-diffusion, while V_{2t} is a pure-jump volatility spike process.	Three jumps, with the last two correlated with V_{1t} and V_{2t} jumps, respectively.
Vjump3	Three-factor additive variance process. V_{1t} follows a jump-diffusion, while V_{2t} and V_{3t} are pure-jump volatility spike processes.	Four jumps, with the last three correlated with V_{1t}, V_{2t}, and V_{3t} jumps, respectively.

All of the above models were estimated with the constraint $\lambda_{j0} = 0$ for $j \leq 1$, based upon evidence in Bates (2006, Table 7) supporting that restriction.[20] In addition, two models Vjump20 and Vjump30 were estimated with $\lambda_{j0} \neq 0$ for $j \leq 1$ and with the self-exciting jumps components suppressed by setting $\lambda_{jj} = 0$ for all $j \geq 1$.

Comparing the models in Table B.I and in Figure 3 indicates two important sources of overall improvement in fit. First is the issue of accurately modeling high frequency price changes of 0 to 5 ticks, which account for 42% of the data. Of primary importance is the introduction in model Vjump1b of a second futures jump component N_{0t} that is uncorrelated with variance jumps. This futures jump component is estimated as a high frequency small amplitude jump component in Vjump1b, and is even higher in frequency and smaller in amplitude for the more general Vjump2 and Vjump3 models (Table B.IV). While observationally equivalent for daily returns to just scaling up diffusive variance V_{1t}, the N_{0t} futures jump component helps model the 15-minute price changes of 0 to 5 ticks more precisely. The adjusted correlation parameter

Figure 3 about here

$$\rho^{adj} \equiv \frac{\rho + \rho_1 \lambda_{11} E(\gamma_{V1}^2)}{\sqrt{\sigma^2 + \lambda_{11} E(\gamma_{V1}^2)}\sqrt{1 + \lambda_{01} E(\gamma_0^2) + \lambda_{11} E(\gamma_1^2)}}. \tag{13}$$

in Table B.III indicates the overall leverage effect: the equivalent of $\rho = Corr(dW_{1t}, dW_{Vt})$ if the $(\gamma_0, \gamma_1, \gamma_{V1})$ shocks were replaced by diffusive shocks with equivalent variances and covariances.

Second is the impact of the 1987 crash. Better modeling of intradaily developments on October 19 and 20 accounts for almost a quarter of the log likelihood improvement in sample of the most general Vjump3 model versus SVJ1 shown in Figure 3. The more general models also fit the fall of 2008 progressively better, indicating the two largest stock market crises over 1983 to 2008 are substantially influencing parameter estimation. Turbulent markets at other times (the first Gulf War, fall 1997, fall 1998, post-9/11/2001) do not appear to have had as distinct an impact

[20] Relaxing this constraint for the Vjump3 model raised the log likelihood from 893,432.73 to 892,438.82 – a small but statistically significant change.

on log likelihood fits. However, log likelihoods are generally increasing throughout the full 1983 to 2008 sample.

The more general models also have better fits out of sample over 2009 to 2016. The progressively better fits of the Vjump1b, Vjump2 and Vjump3 models out of sample are entirely attributable to better modeling of 0 to 3 tick price movements, which similarly account for 42% of observed E-mini price changes. A further breakdown in Table B.II by volatility environment indicates that these models fit all data better regardless of the recent level of realized volatility, both in sample and out of sample. The Vjump20 and Vjump30 models without self-exciting jumps do worse both in sample (mostly during the 1987 crash) and out of sample.

The multifactor Vjump2 and Vjump3 models have progressively richer descriptions of variance dynamics relative to the nested Vjump1b model. In particular, these two models indicate that substantial and self-exciting volatility spikes are an important component of volatility evolution. In the Vjump2 estimates, V_{2t} is typically near zero and has a V_{1t}-dependent intensity that averages out to $\lambda_{20} + \lambda_{21}E(V_{1t})$ = 48 jumps per year. If a variance jump occurs of average size 0.07, V_{2t} increases to $(.265)^2$ and the jump intensity increases by $\lambda_{22}\bar{\gamma}_{V2} = 1486$ jumps/year, or 6 jumps/day. This increase in jump intensity implies that $\lambda_{22}\bar{\gamma}_{V2}/(\beta_2 - \lambda_{22}\bar{\gamma}_{V2}) = 3.0$ additional variance jumps are expected from every average-sized jump in V_{2t}.[21] Furthermore, the positively skewed exponential distribution can have V_{2t} jumps that are two or three times the average jump magnitude $\bar{\gamma}_{V2}$, with corresponding projections of six or nine additional variance jumps. The associated futures price jumps are roughly mean zero, with a standard deviation of 0.36% and a strongly negative correlation (-.92) with the variance jumps. The V_{2t} spikes resulting from variance jumps are highly transient, with an estimated half-life of roughly 1/3 day.

The Vjump3 model decomposes variance jumps into small, medium, and large sizes, with different properties and different associations with the futures returns from which they are filtered.

[21] This calculation is based upon a continuous-time stochastic intensity $\lambda_{2t} = \lambda_{20} + \boldsymbol{\lambda}_{21}V_{1t} + \lambda_{22}V_{2t}$, with reversion rate $\beta_2 - \lambda_{22}\bar{\gamma}_{V2}$ for V_{2t}. The increase in expected future jumps (from an increase in expected future jump intensities) is approximately equal to but less than the number when jump intensities are constant within periods.

The moderately frequent V_{2t} jumps of average size 0.070 in the Vjump2 model are divided further in the Vjump3 model into frequent jumps in V_{2t} of average size 0.022, and rarer jumps in V_{3t} with average size 0.076. The V_{2t} jumps have little self-propagation, die off rapidly within the day (half-life of 0.08 days), and primarily add additional and transient noise to the combined spot variance process $V_{1t} + V_{2t}$. The large and relatively rare V_{3t} jumps have a -0.76 correlation with associated log futures jumps $\gamma_3 \sim [-0.2\%, (1.0\%)^2]$, indicating they are inferred from the largest 15-minute or overnight futures returns. V_{3t} reverts towards zero with a half-life of 1.6 days, implying some spillover across days. Sequences of V_{3t} jumps typically initiate from near zero values of V_{3t}, with a V_{1t}-dependent intensity that averages out to $\lambda_{30} + \lambda_{31}E(V_{1t})$ = 7.4 jumps per year. Conditional upon initiation, each average-sized V_{3t} jump generates an expected additional 4.9 jumps, through its impact on expected future jump intensities.

Let V_{it}^{tot} be the total impact of the state variable V_{it} upon diffusive and jump variance, using the variance factor loadings of Table B.V. Figure 4 graphs the incremental contributions of those total variance components to end of day total spot volatility $(V_{1t}^{tot} + V_{2t}^{tot} + V_{3t}^{tot})^{½}$ over 1983 to 2016. The total estimated number of jumps each day (close to close) is also graphed, using the filtration procedure described above in Section I.C. The graph indicates that major but substantially transient volatility spikes from V_{3t} jumps tend to occur when core volatility $\sqrt{V_{1t}^{tot}}$ is relatively high. Furthermore, the volatility spikes are typically the outcome of *multiple* synchronous jumps in log futures prices and underlying volatility. For instance, the -32.7% change in the log futures price on October 19, 1987 from the previous Friday's closing value was the result of an estimated 34 jumps in V_{3t}. The +5.7% and +17.4% returns on October 20 and 21 were the outcome of 97 and 52 jumps in V_{3t}, respectively. The turbulent and predominantly falling market in the fall of 2008 was similarly the result of multiple intradaily and overnight jumps in V_{2t} and V_{3t} that accompanied predominantly negative stock market jumps.

Figure 4 about here

Figure 5 shows the intradaily evolution of the three factors over October 12 to 30, 1987. A declining stock market over the week of October 12 to16, including an accelerating drop on Friday, October 16, set the stage for the stock market crash of October 19. A volatility spike began

Figure 5 about here

developing late on Friday afternoon, and was stimulated further by the log futures price dropping 5.4% by 9:15 AM on October 19. Substantial intradaily drops over October 19 generated further substantial estimated increases in the volatility spike factor $\sqrt{V_{3t}^{tot}}$, which ended the day at roughly 193% annualized (2.1% per quarter-hour). Major market turbulence on October 20 contributed to further estimated increases in $\sqrt{V_{3t}^{tot}}$, which peaked at 282% annualized (3.1% per quarter-hour) at midday before ultimately declining in the afternoon and on October 21. Log futures prices fell 5% between 9 and 9:15 AM on October 22, prompting another short-lived volatility burst that decayed as the market rebounded and stabilized.

Figure 6 shows the comparable evolution in factors over September and October of 2008. The sharp shocks to the volatility spike factor $\sqrt{V_{3t}^{tot}}$ in September largely reflect various announcements: the government takeover of FNMA and FHLMC announced on September 7, the Lehman Brothers bankruptcy declaration before markets opened on September 15, and the Senate's initial rejection of the Troubled Asset Relief Program (TARP) on September 29. Interesting, the subsequent passage of TARP on October 3 also caused a falling market, and an associated jump in $\sqrt{V_{3t}^{tot}}$. The House of Representatives' vote to approve TARP at 1:27 EST was accompanied by a -0.74% fall in futures prices over 12:15 to 12:30 CST, and a further fall of -1.76% by 12:45. $\sqrt{V_{3t}^{tot}}$ rose immediately, from 5.7% to 9.2% to 44.2% annualized over 12:15 to 12:45. A falling market for the remainder of the day kept $\sqrt{V_{3t}^{tot}}$ high throughout the afternoon. The subsequent week of October 6 to 10 saw a further market decline of 20% and associated high values of volatility. The market remained turbulent throughout the remainder of October.

Figure 6 about here

F. Return diagnostics

Whether the above models are broadly capturing the conditional distributions of returns can be examined by looking at the normalized returns $z_{t+1} = N^{-1}\left[CDF\left(y_{t+1}\middle|\boldsymbol{Y}_t, \widehat{\boldsymbol{\Theta}}\right)\right]$, where $CDF(\cdot)$ is the conditional cumulative distribution function derived from the specified models and computed by Fourier inversion of the associated conditional characteristic functions. Under correct model specification, these residuals are independent draws from a standard Gaussian

distribution. Table I reports in sample summary statistics for z's from various models, while Figure 7 presents related normal probability plots. Normalized returns are computed at two horizons: for intradaily/overnight returns conditional upon past data, and for daily returns (close to close) conditional upon past intradaily and overnight data up through the close of the preceding day. In addition, 100 sample paths of data over 1983 to 2008 were simulated at the estimated parameters and time horizons, and were used to generate 95% confidence intervals for Figure 7.

Figure 7 about here

Table I about here

Table I and Figure 7 indicate that the multifactor models are doing a progressively better job in sample of capturing conditional distributions at the intradaily/overnight frequencies used when estimating the models. The first four moments in all cases are roughly those of a standard normal distribution, although there are statistically significant deviations in all cases. The graphs in the first column of Figure 7 show that the multifactor models Vjump2 and Vjump3 help capture intradaily outliers, which are often substantially sequential. Both models do well for $|z|$-values less than 4, but have some difficulty in capturing the extreme tails ($|z| > 4$). The Vjump2 model underpredicts extreme negative returns while the Vjump3 model overpredicts those returns; and both models underpredict extreme positive returns ($z > 4$) in Figure 7.

The statistics in Table 1 for daily data indicate that the one-factor variance models Vjump1a and Vjump1b have difficulty in capturing the stock market crash of October 19, 1987. Whereas the Vjump1b model partially explains any single 15-minute intradaily outlier, the probability under that model of observing the sequence of outliers that culminated in the overall -32.7% change in log futures prices is low – the equivalent to observing a -7 standard deviation draw from a standard normal distribution. By contrast, the 2-factor model Vjump2 successfully captures the 1987 outlier as a volatility spike that is plausible under the (in sample) parameter estimates. The Vjump3 model does even better at capturing that one day.

Autocorrelation estimates for z and $|z|$ are also given in Table I, as tests of the independence implications of a correctly fitted model. All models have a small but statistically significant negative autocorrelation in intradaily/overnight normalized returns – a result reflecting a small negative autocorrelation in the original log-differenced futures prices. At the daily horizon,

the autocorrelation in normalized returns is smaller, and is not statistically significant. Autocorrelations in absolute normalized returns $|z|$ for intradaily/overnight data are reduced (although still statistically significant) under the multifactor Vjump2 and Vjump3 models, indicating the multifactor models capture intradaily volatility dynamics better. All models have a statistically significant -7% autocorrelation in daily $|z|$, indicating room for improvement in the models' implications for daily volatility dynamics.

II. Realized variance

Define

$$RV_n = \sum_{m=1}^{M_n} \left[\ln\left(F_{n,m}\right) - \ln\left(F_{n,m-1}\right)\right]^2 \tag{14}$$

as the daily realized variance on day *n* from $M_n \leq 26$ sequential intradaily time intervals that begin 15 minutes after pit trading in the S&P 500 futures contract opens, and are typically about 15 minutes in duration. The realized variance literature relies heavily upon the asymptotic convergence of realized variance to quadratic variation as the sampling frequency increases:

$$\begin{aligned} QV_n &\equiv \int_{s=t}^{t+\tau_n^{daily}} (df_s)^2 \\ &= \int_{s=t}^{t+\tau_n^{daily}} \left(\sum_{i=1}^{I} V_{is} ds + \sum_{j=1-K}^{J} \gamma_j^2 dN_{js} \right). \end{aligned} \tag{15}$$

The correlation between realized variance and quadratic variation on simulated Vjump3 data is 95% at the 15-minute horizon, and rises to 98% and 99.7% at 5- and 1-minute horizons, respectively. Because quadratic variation is an affine latent characteristic in affine models, with an analytical conditional characteristic function that is given in Appendix A, examining distributional properties of realized variance as a proxy for those of quadratic variation is another potentially useful diagnostic of the proposed time series models.

The effective length of the intradaily trading period varies on a daily basis, making it desirable to rescale realized variance by the aggregate intradaily time interval

$$252\tau_n^{daily} = \sum_{m=1}^{M_n} 252\tau_{nm} = f_{daily} \exp(\boldsymbol{\beta}_{ID}{}' \boldsymbol{d}_n^{ID}) \tag{16}$$

where $\exp(\boldsymbol{\beta}_{ID}{}' \boldsymbol{d}_n^{ID})$ are the intradaily day of the week effects graphed in Figure 1, and 252 converts the time units from yearly to daily. In particular,

$$Rvol_n = \sqrt{\frac{RV_n}{252\tau_n^{daily}}} \tag{17}$$

is the realized volatility on a daily (24-hour) Wednesday equivalent basis that can be compared to conditional or unconditional volatility assessments from daily close to close returns. The major impact of the daily rescaling is to eliminate the impact of half-days adjacent to holidays, which otherwise look like inliers.

Table II about here

Table II describes characteristics of various transforms of realized volatility, while Figure 8 graphs realized variance and volatility. Realized variance is an extremely skewed and leptokurtic random variable, with especially pronounced outliers during October 19 to 22, 1987. By contrast, a log transform for volatility (or variance) appears substantially better behaved: substantially less pronounced skewness and excess kurtosis in Table II, and more discernable persistence in Figure 8. Indeed, Figure 8 appears to offer significant support for the 2-factor diffusive log variance process estimated on daily data by Chernov et al (2003), in contrast to the affine specifications explored here. However, as discussed in Appendix A.3, this paper's extended DPS volatility jump model does imply a heavy tailed distribution for quadratic variation, which is potentially compatible with the occasional extreme outliers in realized variance.

Figure 8 about here

A Box-Jenkins analysis indicates realized variance follows an ARMA(3,1) process, using a Bayes information criterion for model selection. The statistical reliability of the least squares ARMA estimation methodology is questionable given the extreme nonnormality of realized

variance data. Nevertheless, the result is qualitatively consistent with the Vjump3 model, which implies an ARMA(3, 3) process for quadratic variation.

Table III about here

Table III compares the models' ability to forecast realized variance with two other forecasting methodologies: ARMA forecasts of average intradaily realized variances at 1, 5, and 21 business day horizons, and VIX-based forecasts of average realized variance (including overnight) over 21 business days. For the 1983 to 2008 period used in the original estimations, all Vjump models outperform ARMA-based forecasts, and the more general models do better. All forecasts fit poorly, because of extreme realized variances observed during the 1987 crash.

All forecasts perform comparably at a 1-day horizon over a quieter 1990 to 2008 period that excludes the 1987 crash. The Vjump3 outperforms the simpler models at 5- and 21-day horizons. Unsurprisingly, a VIX-based forecasting methodology outforecasts all of the Vjump models at a 21-day horizon, given options markets have access to more information than forecasts based on past returns. All models have similar forecasting accuracy at 1- and 5-day horizons out of sample over 2009 to 2016. The Vjump3 model of volatility dynamics outperforms the simpler models at a 21-day horizon, and comes close to matching the VIX-based forecasts.

Finally, how well the proposed models match the overall conditional distributions of RV realizations can in principle be evaluated via normal probability plots, in the same fashion used above in Figure 7 for intradaily/overnight and daily returns. Normalized residuals $z_{n+1}^{RV} = N^{-1}\left[CDF^{QV}\left(RV_{n+1}\middle|\boldsymbol{Y}_{n,M_n}, \widehat{\Theta}\right)\right]$ are generated using CDFs evaluated by Fourier inversion of the conditional characteristic function of quadratic variation.

Figure 9 about here

It turns out, however, that conditional distributions of realized variances can differ substantially from those of quadratic variation. Whereas the correlation between 15-minute realized variance and quadratic variation is 95% for data simulated from the Vjump3 model, the correlation of the corresponding *z*-values is only 80%. (The *z* correlations on simulated Vjump3 data rise to 92% and 98% for 5- and 1-minute realized variances, respectively.) Consequently, the graphs in Figure 9 use simulation-based bias corrections and confidence intervals to compare what

should be observed for ordered z_{n+1}^{RV} values with what is actually observed. Similar simulation-based benchmarks are used in Table IV for examining the moments and other characteristics of the z_{n+1}^{RV} values.

Table IV about here

Two results stand out. First, the more general models match the conditional distributions better, when compared with simulation-based benchmarks that correct the biases of the QV-based CDF's. The Vjump2 model substantially reduces the frequency of RV inliers and outliers, relative to the Vjump1b model. The Vjump3 model captures RV outliers event better than the Vjump2 model, but does slightly worse with regard to RV inliers. In all cases, however, the RV realization of $(26.9\%)^2$ on October 20, 1987 remains a major positive outlier.

Second, even the most general Vjump3 model has substantial and statistically significant deviations from simulation benchmarks, in Table IV and Figure 9. While these affine models capture the conditional distributions of daily returns reasonably well, as indicated in Figure 6, there appears to be significant room for improvement in their predictions for the overall conditional distributions of realized variances – especially the frequency of RV inliers. The Vjump3 model does a reasonably good job of capturing median, above median, and extreme RV realizations, however.

III. Option pricing implications

A final criterion of the various models is how well they fit observed option prices. The diagnostics below use implicit volatilities from daily end of day settlement prices of American options on S&P 500 futures over January 1990 to June 2016. Because this paper focuses upon high-frequency properties of stock index returns, I use the shortest maturity available, down to at least one full day before expiration. 1-day serial option prices are typically from the Thursday settlement prior to expiration at Friday's close, while 1-day quarterly option prices are typically from the Wednesday settlement prior to Friday's Special Opening Quotation. Maturities exceeding one month are not examined, because Bates (2012, Table 8) argues that longer-term volatility dynamics not modeled in this paper become important at those horizons.

Similar to AFT (2015), I construct representative prices and associated implicit volatilities for strike prices X_{it} that are integer multiples of the at-the-money implicit volatility:

$$d_{it} \equiv \frac{\ln(X_{it}/F_t)}{IV_t^{atm}\sqrt{T_t}} = 0, \pm 1, \pm 2, ..., \tag{18}$$

where F_t is the futures settlement price and T_t is the option maturity, estimated using the Vjump1b time horizon parameters graphed in Figures 1 and 2. Because of much greater depth in puts than in calls, out-of-the-money put prices are interpolated over a 0 to 6 standard deviation range ($d = \{-6, ..., 0\}$), while call prices are interpolated over a 0 to 2 standard deviation range ($d = \{0,1,2\}$), using the constrained cubic spline interpolation methodology of Bates (1991, 2000).

Any pricing kernel that is affine in the underlying risks implies an affine risk-neutral process that can be used to price European options on futures. This paper uses the following parsimonious pricing kernel discussed in Bates (2006, pp. 944-5):

$$d \ln \mathcal{M}_t = \mu_m dt - R\, d \ln F_t + \boldsymbol{R}_V' d\boldsymbol{V}_t. \tag{19}$$

where the risk premium parameters $\boldsymbol{rp} \equiv (R, \boldsymbol{R}_V)$ determine the compensations for equity, volatility and jump risks. I examine three different parameterizations of $\boldsymbol{rp}$:

1) rp1: the $(R, \boldsymbol{R}_V) = (2.45, \boldsymbol{0})$ parameters from Bates (2012), based upon the estimated sensitivity over 1926 to 2006 of the daily conditional equity premium to $\boldsymbol{V}_t$;
2) rp2: $(R, \boldsymbol{R}_V) > \boldsymbol{0}$, using the best fits to option prices over 1990 to 2008; and
3) rp3: unconstrained $(R, \boldsymbol{R}_V)$, again using the best fits to option prices.

As discussed in Appendix C, the risk premia alter the intensity and average jump sizes of the underlying exponential and Gaussian jumps. The first two specifications imply more frequent and more negative jumps in log futures prices under the risk-neutral measure than under the objective measure. The risk premia also affect the conditional equity premium of futures returns.

This paper uses option pricing fits as an additional diagnostic of the merits of the underlying time series models. Consequently, options are priced *conditional* upon the time series parameter estimates and filtered end-of-day conditional distributions $\hat{g}_{t|t}$ of $\boldsymbol{V}_t$, with fits evaluated using the loss function

$$RMSE(\boldsymbol{rp}) = \sqrt{\frac{1}{NOBS}\sum_{t,i}\left[\frac{\hat{o}\left(F_t, T_t, X_{it}, r_t \middle| \hat{g}_{t|t}, \boldsymbol{rp}\right) - o^B(F_t, T_t, X_{it}, r_t, IV_{it})}{o^B_{IV}(F_t, T_t, X_{it}, r_t, IV_{it})}\right]^2} \qquad (20)$$

where $\hat{o}(\cdot)$ is the model-specific European put or call option price estimate given the inputs,[22] $o^B_{it}(\cdot)$ is the corresponding Black (1976) European futures option price given implicit volatility IV_{it} from interpolated American option prices, and $o^B_{IV}(\cdot)$ is the corresponding option vega. The loss function uses the Broadie, Chernov and Johannes (2007) approach of extrapolating from American to European futures option prices, while the inverse vega weights make the loss function approximately the root mean squared error of estimated versus observed implicit volatilities.

Estimates of $\boldsymbol{rp} = (R, \boldsymbol{R}_V)$ for the rp2 and rp3 specifications were based upon minimizing (20) for standardized option prices over 1990 to 2008, with 2009 to 2016 used for out of sample diagnostics. Three additional criteria were used for assessing the resulting fits:

1. the *level* of the volatility smirk, as measured by IV_t^{atm};
2. the *slope* of the volatility smirk, as measured by the divergence $SKEW_t \equiv IV_t^{call} - IV_t^{put}$ between implicit volatilities of calls and puts that are one standard deviation out-of-the-money; and
3. the log likelihood implications over 1983 to 2016 of the $\boldsymbol{rp}$ estimates for conditional intradaily/overnight equity premia.

The second criterion is the Bates (1991, 1997) skewness premium measure of asymmetry in risk-neutral distributions, expressed in implicit volatility terms. Backus, Foresi, Li and Wu's (1997)

[22] See Bates (2012), Equation (50).

Gram-Charlier approximation indicates that implicit volatilities from options that are one standard deviation out-of-the-money are linearly sensitive to skewness but insensitive to excess kurtosis, making this divergence roughly proportional to risk-neutral skewness.[23]

Results from the various time series models and ***rp*** specifications are in Table V. Overall, more state variables (Vjump1b, …, Vjump3) generally leads to more accurate option prices, with further increases in accuracy when the $(R, \boldsymbol{R}_V)$ parameters are allowed greater flexibility. Overall RMSE drops from 4.41% under the Vjump1b + rp1 specification to 3.63% under the Vjump3 + rp3 specifications.[24] The $(R, \boldsymbol{R}_V)$ parameters for rp3 that best fit option prices yield highly implausible conditional equity premia over 1983 to 2016, whereas the constrained rp1 and rp2 specifications appear innocuous. The implications for risk-neutral parameters are in Table C.I in Appendix C.

Table V about here

Much of the improvement in fits of Vjump3 versus Vjump1b appears attributable to more accurate prediction of the overall level of implicit volatilities, as proxied by IV_t^{atm}. This parallels the results noted above in Table II that the Vjump3 model forecasts future realized variance more accurately at longer horizons than the Vjump2 or Vjump1b models, and approaches the VIX-based forecasts. The Vjump2 model generates the steepest and most accurate predictions of the slope of the volatility smirk.

There is a strong maturity effect to the slope of the volatility smirk that all models largely fail to capture. The volatility smirk typically flattens as options approach maturity. And while the Vjump3/rp2 estimates graphed in Figure 10 are not far off at the 1-day horizon, the estimates do increasingly badly at longer 5- or 18-day horizons. Even the most flexible risk-neutral

Figure 10 about here

[23] Bakshi, Kapadia and Madan (2003) provide a more accurate method of estimating risk-neutral skewness from option prices. However, their approach requires a greater strike price range for calls than is reliably available over 1990 to 2008, whereas calls one standard deviation out of the money are almost always actively traded.

[24] Andersen, Fusari and Todorov (2015) achieve an overall RMSE of 1.40% across all maturities over 1996-2010 for their best-fitting 3-factor model. They, however, are using the Bates (1996, 2000) approach of estimating the risk-neutral parameters and implicit state variables that best match observed option prices, with a penalty if the total daily implicit diffusive variance common to both objective and risk-neutral measures diverges excessively from intradaily nonparametric estimates. This paper by contrast estimates parameters and state variables from past intradaily and overnight futures returns, with only a few additional ***rp*** parameters used to match option prices.

parameterizations under the rp3 specification generally fail to match this maturity effect, as shown in Table VI.

Table VI about here

In sum: the time series models fit observed option prices progressively better as more state variables are added, with Vjump3 achieving the best overall fit. However, there remains a substantial and systematic gap between predicted and observed volatility smirks of less than one month's maturity. Possible explanations include: greater downside jump risk; more aggressive leverage and volatility feedback effects than those modeled in the models; or greater aversion to downside risk than is captured by the pricing kernel specification (19).

The first explanation seems unlikely. Jump-diffusive option pricing models with independent returns such as Bates (1991) or AFT (2017) counterfactually predict the volatility smirk should steepen rather than flatten as options approach maturity. The third explanation has been proposed by Andersen et al (2015) in the form of an additional U-factor inferred from movements in risk-neutral left tail risk that is orthogonal to movements in diffusive variance.

Overall, however, I feel exploring alternative models of leverage and volatility feedback effects is the most promising area for future research. As discussed in Das and Sundaram (1999), a direct relationship between volatility smirks and option maturity at short maturities is suggestive of substantial distributional randomization, such as from stochastic volatility plus leverage. The time series model in equations (1) to (3) is based upon Duffie, Pan and Singleton (2000) because that is the earliest and most tractable volatility jump model. But there are other time series models even within an affine framework (e.g., in AFT (2015)), as well as non-affine models, that that might be more compatible with short-maturity option prices.

IV. Summary

Finite-activity jump-diffusion models such as Merton (1976) posit that log-differenced asset prices are drawn from a mixture of distributions, with major daily outliers the outcome of a draw from a higher-volatility distribution. This model can be viewed as positing instantaneous but instantaneously transitory spikes in intradaily and daily volatility. The intradaily evidence does not support this description of volatility evolution. Instead, large daily market movements are the accumulation over the day of a series of rapid and self-exciting intradaily increases in conditional volatility, typically accompanied by a falling market. Volatility can accelerate rapidly from relatively low levels, and can subside quickly from high levels; but the shifts take time to develop within a given day, and can spill over into subsequent days. These short-lived volatility spikes affect both diffusive and jump volatility, with the former more important. The initiation of a volatility spike is more likely when core volatility is already high.

The central intradaily dynamic proposed and estimated in this paper is self-exciting intradaily volatility spikes that accompany modest and predominantly negative intradaily stock market jumps. The results largely concur with the evidence from the nonparametric realized variance literature that intradaily price jumps tend to be small, with the largest ones in the Vjump3 model having a standard deviation of 1%. Their importance lies more in the dynamic implications; they are a signal that there is immediate risk of more price/volatility co-jumps, and of a run of such jumps that could accumulate into a major daily movement. Runs of successive intradaily price/volatility co-jumps generated the market moves exceeding 10% in magnitude in 1987 and 2008.

REFERENCES

Abramowitz, Milton, and Irene A.Stegun, 1972, *Handbook of Mathematical Functions* (Dover, New York).

Aït-Sahalia, Yacine, Cacho-Diaz, Julio, and Roger J.A. Laeven, 2015, Modeling financial contagion using mutually exciting jump processes, *Journal of Financial Economics* 117, 585-606.

Aït-Sahalia, Yacine, and Jean Jacod, 2014, *High-frequency Financial Economics* (Princeton University Press, Princeton).

Andersen, Torben G., 2004, Discussion [of Barndorff-Nielsen and Shephard (2004)], *Journal of Financial Econometrics* 2, 37-48.

Andersen, Torben G., and Tim Bollerslev, 1997. Intraday periodicity and volatility persistence in financial markets, *Journal of Empirical Finance* 4, 115-158.

Andersen, Torben G., and Tim Bollerslev, 1998, Deutsche mark-dollar volatility: intraday activity patterns, macroeconomic announcements, and longer run dependencies, *Journal of Finance* 53, 219-265.

Andersen, Torben G., Nicola Fusari, and Victor Todorov, 2015, The risk premia embedded in index options, *Journal of Financial Economics* 117, 558-584.

Andersen, Torben G., Nicola Fusari, and Victor Todorov, 2017, Short-term market risks implied by weekly options, *Journal of Finance* 72, 1335-1386.

Backus, David K., Silverio Foresi, Kai Li, and Liuren Wu, 1997, Accounting for biases in Black Scholes, Unpublished manuscript, New York University.

Bakshi, Gurdip, Kapadia, N., and Dilip B. Madan, 2003, Stock return characteristics, skew laws, and the differential pricing of individual equity options, *Review of Financial Studies* 16, 1-101.

Bandi, Federico M., and Roberto Renò, 2016, Price and volatility co-jumps, *Journal of Financial Economics* 119, 107-146.

Barndorff-Nielsen, Ole E., and Neil Shephard, 2004, Power and bipower variation with stochastic volatility and jumps, *Journal of Financial Econometrics* 2, 1-37.

Barndorff-Nielsen, Ole E., and Neil Shephard, 2006, Econometrics of testing for jumps in financial economics using bipower variation, *Journal of Financial Econometrics* 4, 1-30.

Bates, David S., 1991, The crash of '87: was it expected? The evidence from options markets, *Journal of Finance* 46, 1009-1044.

Bates, David S., 1996, Jumps and stochastic volatility: exchange rate processes implicit in deutsche mark options, *Review of Financial Studies* 9, 69-107.

Bates, David S., 1997, The skewness premium: option pricing under asymmetric processes, *Advances in Futures and Options Research* 9, 51-82.

Bates, David S., 2000, Post-'87 crash fears in the S&P 500 futures option market, *Journal of Econometrics* 94, 181-238.

Bates, David S., 2006, Maximum likelihood estimation of latent affine processes, *Review of Financial Studies* 19, 909-965.

Bates, David S., 2012, U.S. stock market crash risk, 1926-2010, *Journal of Financial Economics* 105, 229-259.

Black, Fischer, 1976, The pricing of commodity contracts, *Journal of Financial Economics* 3, 167-179.

Broadie, Mark N., Mikhail Chernov, and Michael Johannes, 2007, Model specification and risk premiums: evidence from futures options, *Journal of Finance* 62, 1453-1490.

Calvet, Laurent, and Adlai J. Fisher, 2008, *Multifractal volatility: theory, forecasting, and pricing* (Academic Press, Amsterdam).

Campbell, John Y., Andrew W. Lo, and A. Craig MacKinlay, A.C., 1997. *The Econometrics of Financial Markets*. Princeton University Press.

Carlson, Mark, 2006, A brief history of the 1987 stock market crash with a discussion of the Federal Reserve response, Unpublished manuscript, Board of Governors of the Federal Reserve.

Carr, Peter, and Liuren Wu, 2008, Leverage effect, volatility feedback, and self-exciting market disruptions: disentangling the multi-dimensional variations in S&P 500 index options, Unpublished manuscript, Baruch College.

Chan, Kalok, K. C. Chan, and G. Andrew Karolyi, 1991, Intraday volatility in the stock index and stock index futures market, *Review of Financial Studies* 4, 657-684.

Chernov, Mikhail, A. Ronald Gallant, Eric Ghysels, and George Tauchen, 2003, Alternative models for stock price dynamics, *Journal of Econometrics* 116, 225-257.

Das, Sanjiv R., and Rangarajan K. Sundaram, 1999, Of smiles and smirks: a term-structure perspective, *Journal of Financial and Quantitative Analysis* 34, 211-239.

Duffie, Darrell, Jun Pan, and Kenneth J. Singleton, 2000, Transform analysis and asset pricing for affine jump-diffusions, *Econometrica* 68, 1343-1376.

Eraker, Bjorn, Michael Johannes, and Nicholas G. Polson, 2003, The impact of jumps in volatility and returns, *Journal of Finance* 58, 1269-300.

Fulop, Andras, Junye Li, and Jun Yu, 2015, Self-exciting jumps, learning, and asset pricing implications, *Review of Financial Studies* 28, 876-912.

Gallant, A. Ronald, 1981, On the bias in flexible functional forms and an essentially unbiased form: The Fourier flexible form, *Journal of Econometrics* 15, 211-245.

Hausman, Jerry A., Andrew W. Lo, and A. Craig MacKinlay, 1992, An ordered probit analysis of transaction stock prices, *Journal of Financial Economics* 31, 319-379.

Heston, Steve L., 1993, A closed-form solution for options with stochastic volatility with applications to bond and currency options, *Review of Financial Studies* 6, 327-344.

Huang, Zin, and George Tauchen, 2005, The relative contribution of jumps to total price variance, *Journal of Financial Econometrics* 3, 456-499.

Jacod, Jean, and Victor Todorov, 2010, Do price and volatility jump together? *Annals of Applied Probability* 20, 1425-1469.

Jones, Christopher S., 2003, The dynamics of stochastic volatility: evidence from underlying and options markets, *Journal of Econometrics* 116, 147-180.

Lee, Suzanne S., and Per A. Mykland, 2008, Jumps in financial markets: a new nonparametric test and jump dynamics, *Review of Financial Studies* 21, 2535-2563.

Mancini, Cecilia, 2009, Nonparametric threshold estimation for models with stochastic diffusion coefficient and jumps, *Scandinavian Journal of Statistics* 36, 270-296.

Merton, Robert C., 1976. Option pricing when underlying stock returns are discontinuous. *Journal of Financial Economics* 3, 125-144.

Poppe, G.P.M., and C.M.J. Wijers, 1990, More efficient computation of the complex error function, *ACM Transactions on Mathematical Software* 16, 38-46.

Prokopczuk, Marcel, and Chardin Wese Simen, 2014, What makes the market jump? Unpublished manuscript, Leibniz University Hannover.

Stroud, Jonathan R., and Michael Johannes, 2014, Bayesian modeling and forecasting of 24-hour high-frequency volatility, *Journal of the American Statistical Association* 109, 1368-1384.

Tauchen, George, and Hao Zhou, 2011, Realized jumps on financial markets and predicting credit spreads, *Journal of Econometrics* 160, 102-118.

Appendix A

A.1 Joint characteristic functions for futures prices, spot variance, and other latent variables

The fundamental building blocks for the multifactor and multi-jump models in this paper are based on the single-factor Duffie, Pan, and Singleton (2000) model, which has constant-intensity synchronous correlated jumps in the log futures prices f_t and underlying spot variance V_t. Let x_t be some additional latent variable of interest; e.g., the accumulated number or size of jumps, or quadratic variation and its integrated variance and squared jump components. Each of these variables follows a pure jump process, implying (f_t, V_t, x_t) evolve as

$$\begin{aligned} df_t &= [\mu_0 + (\mu_1 - ½)V_t]dt + \sqrt{V_t}dW_t + (\gamma dN_t - \lambda\bar{k}dt) \\ dV_t &= (\alpha - \beta V_t)dt + \sigma\sqrt{V_t}dW_{Vt} + \gamma_V dN_t \\ dx_t &= \mu_x V_t dt + \gamma_x dN_t. \end{aligned} \tag{A.1}$$

W_t and W_{Vt} are Wiener processes with correlation ρ, N_t is a Poisson counter with constant intensity λ, $\gamma_V \sim Exp(\bar{\gamma}_V)$ is the exponentially distributed jump in spot variance conditional upon a jump, and $\gamma = \rho_J\gamma_V + \gamma_f$ for $\gamma_f \sim N(\bar{\gamma}_f, \delta_f^2)$ is the correlated jump in log futures prices conditional upon a jump, with expected percentage jump size $\bar{k} = Ee^{\gamma} - 1 = e^{\bar{\gamma}_f + ½\delta_f^2}/(1 - \rho_J\bar{\gamma}_V) - 1$. Specific processes for x_t will be discussed further below.

The generalized Fourier transform for future $\boldsymbol{z}_{t+\tau} = (f_{t+\tau}, V_{t+\tau}, x_{t+\tau})$ and complex $(\boldsymbol{\Phi}, \boldsymbol{\psi}, \boldsymbol{\xi})$ conditional upon current $\boldsymbol{z}_t$ is

$$\begin{aligned} &\mathcal{F}(\tau; \boldsymbol{\Phi}, \boldsymbol{\psi}, \boldsymbol{\xi} | \boldsymbol{z}_t) \equiv E[\exp(\boldsymbol{\Phi} f_{t+\tau} + \boldsymbol{\psi} V_{t+\tau} + \boldsymbol{\xi} x_{t+\tau}) \mid \boldsymbol{z}_t] \\ &= \exp[\boldsymbol{\Phi} f_t + \boldsymbol{\xi} x_t + C(\tau; \boldsymbol{\Phi}, \boldsymbol{\psi}, \boldsymbol{\xi}) + D(\tau; \boldsymbol{\Phi}, \boldsymbol{\psi}, \boldsymbol{\xi})V_t + \lambda E(\tau; \boldsymbol{\Phi}, \boldsymbol{\psi}, \boldsymbol{\xi})\,]. \end{aligned} \tag{A.2}$$

$\mathcal{F}(\cdot)$ solves the backward Kolmogorov equation $E_t d\mathcal{F}(\cdot) = 0$ associated with (A.1), implying that $C(\tau; \cdot)$, $D(\tau; \cdot)$ and $E(\tau; \cdot)$ solve the following system of ordinary differential equations subject to $C(0; \cdot) = E(0; \cdot) = 0$ and $D(0; \cdot) = \boldsymbol{\psi}$:

$$
\begin{aligned}
C_\tau &= \mu_0 \boldsymbol{\Phi} + \alpha D \\
D_\tau &= N(\boldsymbol{\Phi}, \boldsymbol{\xi}) + M(\boldsymbol{\Phi}) D + \tfrac{1}{2}\sigma^2 D^2 \\
E_\tau &= E\left[e^{\boldsymbol{\Phi}(\gamma_f + \rho_J \gamma_V) + D(\tau;\cdot)\gamma_V + \xi \gamma_x}\right] - 1 - \boldsymbol{\Phi}\bar{k}
\end{aligned}
\tag{A.3}
$$

where $N(\boldsymbol{\Phi}, \boldsymbol{\xi}) = \tfrac{1}{2}\boldsymbol{\Phi}^2 + (\mu_1 - \tfrac{1}{2})\boldsymbol{\Phi} + \mu_x \boldsymbol{\xi}$ and $M(\boldsymbol{\Phi}) = \rho\sigma\boldsymbol{\Phi} - \beta$. $\boldsymbol{\xi}$ is used when estimating the latent characteristic $x_{t+\tau} - x_t$, and is otherwise set to zero. The solution for $D(\tau; \cdot)$ is[25]

$$
D(\tau; \boldsymbol{\Phi}, \boldsymbol{\psi}, \boldsymbol{\xi}) = \frac{2N(\boldsymbol{\Phi}, \boldsymbol{\xi}) + \boldsymbol{\psi}[M(\boldsymbol{\Phi}) + R(\tau, \boldsymbol{\Phi}, \boldsymbol{\xi})]}{R(\tau, \boldsymbol{\Phi}, \boldsymbol{\xi}) - M(\boldsymbol{\Phi}) - \sigma^2 \boldsymbol{\psi}} \tag{A.4}
$$

where

$$
\begin{aligned}
R(\tau, \boldsymbol{\Phi}, \boldsymbol{\xi}) &= \gamma(\boldsymbol{\Phi}, \boldsymbol{\xi}) \frac{e^{\gamma(\boldsymbol{\Phi}, \boldsymbol{\xi})\tau} + 1}{e^{\gamma(\boldsymbol{\Phi}, \boldsymbol{\xi})\tau} - 1} \text{ and} \\
\gamma(\boldsymbol{\Phi}, \boldsymbol{\xi}) &= \sqrt{M(\boldsymbol{\Phi})^2 - 2\sigma^2 N(\boldsymbol{\Phi}, \boldsymbol{\xi})}.
\end{aligned}
\tag{A.5}
$$

The solution for $C(\tau; \cdot)$ is

$$
\begin{aligned}
C(\tau; \boldsymbol{\Phi}, \boldsymbol{\psi}, \boldsymbol{\xi}) = \mu_0 \Phi \tau &- \frac{\alpha\tau}{\sigma^2}[M(\boldsymbol{\Phi}) - \gamma(\boldsymbol{\Phi}, \boldsymbol{\xi})] \\
&- \frac{2\alpha}{\sigma^2} \ln\left\{1 + [M(\boldsymbol{\Phi}) - \gamma(\boldsymbol{\Phi}, \boldsymbol{\xi})] \frac{1 - e^{\gamma(\boldsymbol{\Phi}, \boldsymbol{\xi})\tau}}{2\gamma(\boldsymbol{\Phi}, \boldsymbol{\xi})}\right\} \\
&- \frac{2\alpha}{\sigma^2} \ln\left[1 - \frac{\sigma^2 \boldsymbol{\psi}}{R(\tau, \boldsymbol{\Phi}, \boldsymbol{\xi}) - M(\boldsymbol{\Phi})}\right].
\end{aligned}
\tag{A.6}
$$

The solution for $E(\tau; \cdot)$ depends upon the specification of the jump distribution γ_x of x_t. For the benchmark model with $\boldsymbol{\xi} = 0$ that is used when filtering and estimating models,

[25] If jumps have stochastic intensity $\lambda_t = \lambda + \lambda_1 V_t$, then $D(\tau; \cdot)$ solves $D_\tau = N + MD + \tfrac{1}{2}\sigma^2 D^2 + \lambda_1 E_\tau[D(\cdot); \cdot]$. This is of cubic rather than quadratic order when $\boldsymbol{\xi} = 0$, and has an implicit but not explicit solution for $D(\tau; \cdot)$, precluding rapid evaluation. Such models typically are solved numerically; e.g., Carr and Wu (2008).

$$E(\tau;\boldsymbol{\Phi},\boldsymbol{\psi},0) = e^{\boldsymbol{\Phi}\bar{\gamma}_f+\frac{1}{2}\boldsymbol{\Phi}^2\delta_f^2}\left\{\frac{b}{d}\tau - e\ln\left[1+\frac{c\left(e^{-\gamma(\boldsymbol{\Phi},\boldsymbol{\xi})\tau}-1\right)}{c+d}\right]\right\} - \left(1+\boldsymbol{\Phi}\bar{k}\right)\tau \equiv H(\tau;\boldsymbol{\Phi},\boldsymbol{\psi}) - \left(1+\boldsymbol{\Phi}\bar{k}\right)\tau \quad \text{(A.7)}$$

where

$$\begin{aligned} b &= [M(\boldsymbol{\Phi}) - \gamma(\boldsymbol{\Phi},\boldsymbol{\xi})] + \sigma^2\boldsymbol{\psi} \\ c &= \{-s[M(\boldsymbol{\Phi}) + \gamma(\boldsymbol{\Phi},\boldsymbol{\xi})] - 2\bar{\gamma}_V N(\boldsymbol{\Phi},\boldsymbol{\xi})]\} + \boldsymbol{\psi}\{-s\sigma^2 \\ &\quad - \bar{\gamma}_V[M(\boldsymbol{\Phi}) - \gamma(\boldsymbol{\Phi},\boldsymbol{\xi})]\} \\ d &= \{s[M(\boldsymbol{\Phi}) - \gamma(\boldsymbol{\Phi},\boldsymbol{\xi})] + 2\bar{\gamma}_V N(\boldsymbol{\Phi},\boldsymbol{\xi})]\} + \boldsymbol{\psi}\{s\sigma^2 \\ &\quad + \bar{\gamma}_V[M(\boldsymbol{\Phi}) + \gamma(\boldsymbol{\Phi},\boldsymbol{\xi})]\} \\ e &= \frac{2\bar{\gamma}_V}{2\bar{\gamma}_V^2 N(\boldsymbol{\Phi},\boldsymbol{\xi}) + 2\bar{\gamma}_V M(\boldsymbol{\Phi})s + \sigma^2 s^2} \text{ and} \\ s &= 1 - \rho_J\bar{\gamma}_V\boldsymbol{\Phi}. \end{aligned} \quad \text{(A.8)}$$

When x_t is the accumulated number or size of jumps, or the integrated variance, $E(\tau;\cdot)$ takes the following forms, for $H(\cdot)$ defined above in (A.7):

x_t	μ_x	γ_x	$E(\tau;\boldsymbol{\Phi},\boldsymbol{\psi},\boldsymbol{\xi})$
N_t	0	1	$e^{\xi}H(\tau;\boldsymbol{\Phi},\boldsymbol{\psi}) - \left(1+\boldsymbol{\Phi}\bar{k}\right)\tau$
$\int_0^t \gamma dN_s$	0	γ	$H(\tau;\boldsymbol{\Phi}+\boldsymbol{\xi},\boldsymbol{\psi}) - \left(1+\boldsymbol{\Phi}\bar{k}\right)\tau$
$\int_0^t \gamma_V dN_s$	0	γ_V	$H(\tau;\boldsymbol{\Phi},\boldsymbol{\psi}+\boldsymbol{\xi}) - \left(1+\boldsymbol{\Phi}\bar{k}\right)\tau$
$\int_0^t V_s ds$	1	0	$H(\tau;\boldsymbol{\Phi},\boldsymbol{\psi}) - \left(1+\boldsymbol{\Phi}\bar{k}\right)\tau$

For quadratic variation $x_t = \int_0^t (V_s ds + \gamma^2 dN_s)$, or its squared jump subcomponent, the jump size $\gamma_x = \gamma^2 = \left(\gamma_f + \rho_{sv}\gamma_V\right)^2$. This has a heavy-tailed distribution when γ_V is exponentially distributed, with infinite values for the moment generating function $E\left[e^{\xi\gamma^2}\right]$ when ξ is real and

positive. Quadratic variation is consequently also heavy-tailed for the DPS process, although the conditional characteristic function and moments of all orders exist. Integrating successively over the independent Gaussian and exponential distributions of γ_f and γ_V, the generalized transform of the jump components is

$$\begin{aligned}\mathcal{F}^J(\boldsymbol{\Phi},\boldsymbol{\psi},\boldsymbol{\xi}) &\equiv E\exp\left[\boldsymbol{\Phi}\left(\gamma_f+\rho_{sv}\gamma_V\right)+\boldsymbol{\psi}\gamma_V+\boldsymbol{\xi}\left(\gamma_f+\rho_{sv}\gamma_V\right)^2\right] \\ &= \frac{E\{\exp[a(\boldsymbol{\xi})\gamma_V^2+b(\boldsymbol{\Phi},\boldsymbol{\psi},\boldsymbol{\xi})\gamma_V+c(\boldsymbol{\Phi},\boldsymbol{\xi})]\}}{\sqrt{1-2\delta_f^2\boldsymbol{\xi}}} \\ &= \frac{e^{c(\boldsymbol{\Phi},\boldsymbol{\xi})}}{2\bar{\gamma}_V}\sqrt{\frac{-\pi}{\rho_{sv}^2\boldsymbol{\xi}}}\,w\left(d(\boldsymbol{\xi})\frac{b(\boldsymbol{\Phi},\boldsymbol{\psi},\boldsymbol{\xi})\bar{\gamma}_V-1}{2\bar{\gamma}_V\sqrt{a(\boldsymbol{\xi})}}\right)\end{aligned} \tag{A.9}$$

where

$$\begin{aligned}a(\boldsymbol{\xi}) &= \frac{\rho_{sv}^2\boldsymbol{\xi}}{1-2\delta_f^2\boldsymbol{\xi}} \\ b(\boldsymbol{\Phi},\boldsymbol{\psi},\boldsymbol{\xi}) &= \boldsymbol{\psi}+\frac{\rho_{sv}(\boldsymbol{\Phi}+2\bar{\gamma}_f\boldsymbol{\xi})}{1-2\delta_f^2\boldsymbol{\xi}} \\ c(\boldsymbol{\Phi},\boldsymbol{\xi}) &= \frac{½\delta_f^2\boldsymbol{\Phi}^2+\bar{\gamma}_f\boldsymbol{\Phi}+\bar{\gamma}_f^2\boldsymbol{\xi}}{1-2\delta_f^2\boldsymbol{\xi}} \\ d(\boldsymbol{\xi}) &= Sign\{Im[a(\boldsymbol{\xi})]\}=\pm1\end{aligned} \tag{A.10}$$

and $w(\boldsymbol{z})$ for complex-valued $\boldsymbol{z}$ is the Fadeeva or plasma-dispersion function (equation 7.1.3 in Abramowitz and Stegun (1972, p.297)). It is a scaled version of the complex complementary error function ($w(\boldsymbol{z})=e^{-\boldsymbol{z}^2}erfc(-i\boldsymbol{z})$), and can be evaluated using algorithm 680 of Poppe and Wijers (1990).[26] Equation (A.9) is well-defined for complex-valued $\boldsymbol{\xi}$ provided $Re[a(\boldsymbol{\xi})]<0$ – which is *not* true for small positive real values of ξ. The jump term $E(\tau;\boldsymbol{\Phi},\boldsymbol{\psi},\boldsymbol{\xi})$ in (A.2) and (A.3) that is

[26]Poppe and Wijers' algorithm is accurate to 14 significant digits, whereas the complex-valued Faddeva function ZERFE in IMSL is accurate to only 10 digits. Furthermore, ZERFE does not appear to be fully reliable for all values of $\boldsymbol{\xi}$, when compared with direct numerical integration over the exponential density of γ_V.

used for estimating latent quadratic variation or its squared jump component given parameter estimates can then be computed numerically:

$$E(\tau;\boldsymbol{\Phi},\boldsymbol{\psi},\boldsymbol{\xi}) = \int_{s=0}^{\tau} \mathcal{F}^J(\boldsymbol{\Phi}, D(s;\cdot),\boldsymbol{\xi})\, ds - \left(1+\boldsymbol{\Phi}\bar{k}\right)\tau. \tag{A.11}$$

I use 9-point trapezoidal integration in the QV-based diagnostics of realized variance.

A.2 Multiple state variables

Because all state variables V_{it} are assumed to evolve independently intraperiod, log characteristic functions are the sum of the log characteristic functions associated with each V_{it}. Define $\boldsymbol{\Theta}_i^{diff} = (\mu_i, \alpha_i, \beta_i, \sigma_i, \rho_i; \mu_{xi})$ as the diffusive parameters associated with the variance process V_{it} and latent characteristic x_{it}, and define $\boldsymbol{\Theta}_j^{jump} = \left(\bar{\gamma}_{Vj}, \rho_j, \bar{\gamma}_{fj}, \delta_j\right)$ as the jump parameters associated with jump process N_{jt}. Define $C_i(\tau;\boldsymbol{\Phi},\boldsymbol{\psi}_i,\boldsymbol{\xi}_i)$ and $D_i(\tau;\boldsymbol{\Phi},\boldsymbol{\psi}_i,\boldsymbol{\xi}_i)$ as equations (A.6) and (A.4) evaluated at parameter values $\boldsymbol{\Theta}_i^{diff}$. For $i > 1$, $(\alpha_i, \sigma_i, \rho_i) = \mathbf{0}$ and $C_i = 0$. Define $E_j(\tau;\boldsymbol{\Phi},\boldsymbol{\psi}_j,\xi_j)$ for $j > 0$ as the relevant above expression for $E(\tau;\boldsymbol{\Phi},\boldsymbol{\psi}_j,\xi_j)$ evaluated at $(\boldsymbol{\Theta}_j^{diff}, \boldsymbol{\Theta}_i^{jump})$. Finally, let $E_0(\tau;\boldsymbol{\Phi},\boldsymbol{\xi}_0)$ be the solution in the simpler special case associated with jump process N_{0t}, for futures jumps that are unaccompanied by volatility jumps Because jump intensities are assumed constant intraperiod, the generalized Fourier transform for future $\boldsymbol{z}_{t+\tau} = (f_{t+\tau}, \boldsymbol{V}_{t+\tau}, \boldsymbol{x}_{t+\tau})$ conditional upon current $\boldsymbol{z}_t$ is a multifactor extension of (A.2):

$$\begin{aligned}
&\mathcal{F}(\tau;\boldsymbol{\Phi},\boldsymbol{\psi},\boldsymbol{\xi}|\,\boldsymbol{z}_t) \;\equiv\; E[\exp(\boldsymbol{\Phi} f_{t+\tau} + \boldsymbol{\psi}'\boldsymbol{V}_{t+\tau} + \boldsymbol{\xi}'\boldsymbol{x}_{t+\tau})|\,\boldsymbol{z}_t] \\
&= \exp\Bigg[\boldsymbol{\Phi} f_t + \mu_0\boldsymbol{\Phi}\tau + \boldsymbol{\xi}'\boldsymbol{x}_t + \sum_{i=1}^{I}[C_i(\tau;\boldsymbol{\Phi},\boldsymbol{\psi}_i,\boldsymbol{\xi}_i) + D_i(\tau;\boldsymbol{\Phi},\boldsymbol{\psi}_i,\boldsymbol{\xi}_i)V_{it}] \\
&\qquad + \lambda_{01}V_{1t}E_0(\tau;\boldsymbol{\Phi},\boldsymbol{\xi}_0) \;+ \sum_{j=1}^{J}\left(\lambda_{j0} + \boldsymbol{\lambda}_j'\boldsymbol{V}_t\right)E_j(\tau;\boldsymbol{\Phi},\boldsymbol{\psi}_j,\boldsymbol{\xi}_j)\Bigg].
\end{aligned} \tag{A.12}$$

A.3 Time aggregation

The key modification in this paper relative to DPS (2000) is to allow jump intensities to vary across periods, while maintaining the DPS assumption of a constant intraperiod jump intensity. By iterating expectations over (A.12) progressively backwards in time, the multiperiod conditional cumulant generating function takes the affine concatenated form

$$\begin{aligned}&\ln E\left[e^{\boldsymbol{\Phi}(f_T-f_t)+\boldsymbol{\psi}'\boldsymbol{V}_T+\boldsymbol{\xi}'(\boldsymbol{x}_T-\boldsymbol{x}_t)}|\boldsymbol{V}_t\right]\\&\qquad=\mu_0\boldsymbol{\Phi}(T-t)+\sum_{i=1}^{I}C_{t,T}^{i}(\boldsymbol{\Phi},\boldsymbol{\psi},\boldsymbol{\xi})+D_{t,T}^{i}(\boldsymbol{\Phi},\boldsymbol{\psi},\boldsymbol{\xi})V_{it}.\end{aligned}\tag{A.13}$$

Its components satisfy the backwards recursion

$$\begin{aligned}D_{t,T}^{1}&=D_1\left(\tau_t;\boldsymbol{\Phi},D_{t+1,T}^{1},\boldsymbol{\xi}_1\right)+\lambda_{01}E_0(\tau_t;\boldsymbol{\Phi},\boldsymbol{\xi}_0)+\sum_{j=1}^{J}\lambda_{j1}E_1(\tau_t;\boldsymbol{\Phi},D_{t+1,T}^{1},\boldsymbol{\xi}_j)\\D_{t,T}^{i}&=D_i\left(\tau_t;\boldsymbol{\Phi},D_{t+1,T}^{i},\boldsymbol{\xi}_i\right)+\lambda_{ii}E_i\left(\tau_t;\boldsymbol{\Phi},D_{t+1,T}^{i},\boldsymbol{\xi}_i\right)\ for\ i>1\\C_{t,T}^{i}&=C_{t+1,T}^{i}+C_i\left(\tau;\boldsymbol{\Phi},D_{t+1,T}^{i},\boldsymbol{\xi}_i\right)+\lambda_{i0}E_i\left(\tau;\boldsymbol{\Phi},D_{t+1,T}^{i},\boldsymbol{\xi}_i\right)\ for\ i\geq 1\end{aligned}\tag{A.14}$$

subject to the terminal condition $(C_{T,T}^{i},D_{T,T}^{i})=(0,\boldsymbol{\psi}_i)$ for $i=1,\ldots,I$. If overnight periods are omitted, as in the cumulant generating function associated with *N*-day future intradaily quadratic variation, the relevant $\boldsymbol{\xi}_j$'s are set to zero on overnight periods within the recursion.

Appendix B: Estimates of the Log Futures Price Process

$$
\begin{aligned}
df_t &= \mu_0 dt + \sum_{i=1}^{I}\left[(\mu_i - ½)V_{it}dt + \sqrt{V_{it}}dW_{it}\right] + \sum_{j=1-K}^{J}\gamma_j dN_{jt} - \lambda_{jt}\bar{k}_j dt \\
dV_{1t} &= (\alpha - \beta_1 V_{1t})dt + \sigma\sqrt{V_{1t}}dW_{Vt} + \gamma_{V1}dN_{1t} \\
dV_{it} &= -\beta_i V_{it}dt + \gamma_{Vi}dN_{it} \text{ for } i > 1
\end{aligned}
\tag{B.1}
$$

I is the number of state variables in $\boldsymbol{V}_t$, J is the number of synchronous jumps in spot variance and futures prices, and K is the number of jumps in futures prices only. Diffusive shocks dW_{1t} and dW_{Vt} have correlation ρ, while the intraperiod jump intensities λ_{jt} of Poisson counter N_{jt} are given below in Table B.IV.

Table B.I
Log Likelihoods of Various Models

Model	I	J	K	Number of parameters	ln L	Δ ln L 0-5 ticks	Δ ln L >5 ticks	Δ ln L All
In sample SP futures (1983-2008)								
SVJ1	1	0	1	28	891,425.32			
Vjump1a	1	1	0	30	892,063.47	740.48	-102.32	638.16
Vjump1b	1	1	1	33	892,575.37	1533.22	-1021.32	511.90
Vjump2	2	2	1	42[a]	893,212.58	255.16	382.05	637.21
Vjump3	3	3	1	51[a]	893,432.73	146.89	73.24	220.13
Vjump20	2	2	1	41[a]	892,940.09	-550.57[b]	286.08[b]	-264.49[b]
Vjump30	3	3	1	49[a]	893,211.30	-311.13[b]	89.71[b]	-221.42[b]

Out of sample E-minis (2009-16)	ln L	Δ ln L 0-3 ticks	Δ ln L >3 ticks	Δ ln L All
SVJ1	264,883.15			
Vjump1a	264,849.78	-80.79	47.48	-33.31
Vjump1b	265,044.26	660.18	-499.01	161.17
Vjump2	265,196.38	900.44	-587.14	313.30
Vjump3	265,261.23	1040.69	-662.55	378.14
Vjump20[b]	265,109.41	-313.42	226.44	-86.97
Vjump30[b]	265,160.85	-311.13	187.21	-100.38

[a]Multifactor models use the Vjump1b estimates of overnight/intradaily and diurnal seasonals.
[b]Δ ln L for Vjump20 and Vjump30 are relative to the Vjump2 and Vjump3 fits, respectively.

Table B.II
Changes in Log Likelihoods Relative to Simpler Models
Conditional on the Previous Day's Realized Volatility

Tercile breakpoints for realized volatility over 1983-2016 are 0.62% and 0.96%.

	1983-2008			2009-16		
RV_{n-1} **tercile**	**Low**	**Medium**	**High**	**Low**	**Medium**	**High**
% of sample	**30%**	**38%**	**33%**	**46%**	**29%**	**25%**
Vjump1a	281.80	232.28	123.70	40.56	-30.63	-42.85
Vjump1b	246.14	145.60	120.68	120.55	51.88	22.30
Vjump2	161.31	148.80	326.61	84.16	12.90	55.33
Vjump3	67.53	78.58	73.52	40.01	23.11	1.95
Vjump20[a]	-84.30	-0.99	-179.61	-101.95	5.58	8.51
Vjump30[a]	-64.78	-44.14	-112.88	-79.05	-6.39	-16.18

[a] $\Delta \ln L$ for Vjump20 and Vjump30 are relative to the Vjump2 and Vjump3 fits.

Table B.III
Parameter Estimates for Specific Models

Parameter estimates are generally on an annualized basis, with Tuesday close to Wednesday close equal to 1/252 years. The half-lives $HL_i = 252\,(\ln 2)\,/(\beta_i - \lambda_{ii}\bar{\gamma}_{Vi})$ to variance shocks are reported in days. ρ^{adj} is the value of $\rho = Corr(dW_{1t}, dW_{Vt})$ if the jumps $(\gamma_0, \gamma_1, \gamma_{V1})$ are replaced with diffusive equivalents.

	Vjump1a	Vjump1b	Vjump2		Vjump3		
	V_{1t}	V_{1t}	V_{1t}	V_{2t}	V_{1t}	V_{2t}	V_{3t}
Conditional mean							
μ_0	-.10	-.08	-.08		.01		
	(.02)	(.03)	(.04)		(.04)		
μ_i	8.0	8.0	5.9	7.4	2.5	1.9	0.3
	(1.5)	(2.5)	(4.3)	(2.95)	(9.0)	(11.7)	(3.7)
Variance processes							
$\sqrt{E(V_i)}$	.155	.131	.108	.082	.092	.070	.071
	(.003)	(.003)	(.003)	(.004)	(.004)	(.004)	(.009)
HL_i (days)	3.6	5.2	9.4	0.35	13.4	0.08	1.6
	(0.2)	(0.3)	(0.7)	(0.03)	(1.1)	(0.01)	(0.4)
σ	.47	.51	.26		.19		
	(.05)	(.02)	(.03)		(.03)		
ρ	-.70	-.63	-.81		-.99		
	(.07)	(.03)	(.08)		(.13)		
ρ^{adj}		-.52	-.60		-.69		
		(.02)	(.03)		(.42)		

Table B.IV
Jump Parameters from Specific Models

The log futures jump sizes and annualized jump intensities for Poisson counter N_{jt} are

$$\gamma_j = \rho_J \gamma_{Vj} + \gamma_{fj} \sim (\bar{\gamma}_j, \delta_j^2)$$

$$\lambda_{jt} = \begin{cases} \lambda_{j1} V_{1t^*} & \text{for } j \leq 1 \\ \lambda_{j0} + \lambda_{j1} V_{1t^*} + \lambda_{jj} V_{jt^*} & \text{for } j > 1 \end{cases}$$

where $\gamma_{Vj} \sim Exp(\bar{\gamma}_{Vj})$ is the synchronous jump in annualized diffusive variance V_{jt}, γ_{fj} is an independent Gaussian shock, and the V_{jt^*}'s are variances at the start of the period. Log futures price jumps have correlation $Corr_j = \rho_j \bar{\gamma}_{Vj}/\delta_j$ with variance jumps, with no variance jumps ($\bar{\gamma}_{V0} = 0$) for Poisson counter N_{0t}. The γ_j parameters are in basis points; $\bar{\gamma}_1$ = -0.051% for the Vjump1a model, with a standard deviation of 0.326%. $E[\Delta N|J]$ is the expected number of additional jumps over a 1-day or infinite horizon conditional upon a variance jump of size $\bar{\gamma}_{Vj}$. Intradaily 15-minute periods were on average 1.20e-4 years, while the unconditional standard deviation of all 15-minute returns over 1983-2008 was 0.19%. Standard errors are in parentheses.

	Vjump1a	Vjump1b	
	N_{1t}	N_{0t}	N_{1t}
λ_{j0}			
$\lambda_{j1} \times 10^{-4}$		38.3	
		(3.7)	
$\lambda_{jj} \times 10^{-4}$	2.0		0.31
	(0.1)		(0.02)
$\bar{\gamma}_j \times 10^4$	-5.1	-1.0	-20.4
	(0.7)	(0.1)	(4.0)
$\delta_j \times 10^4$	32.6	11.4	90.2
	(0.6)	(0.3)	(2.7)
$\bar{\gamma}_{Vj}$	.0063		.0115
	(.0002)		(.0006)
ρ_j	-.27		-.49
	(.01)		(.03)
$Corr_j$	-.52		-.62
	(.02)		(.03)
$E[\Delta N^{\text{day}}\|J]$	0.46	16.4	0.13
	(0.02)	(1.4)	(0.01)
$E[\Delta N^{\infty}\|J]$	2.63	131	1.05
	(0.16)	(14)	(0.09)

Table B.IV (continued)

	Vjump2			Vjump3			
	N_{0t}	N_{1t}	N_{2t}	N_{0t}	N_{1t}	N_{2t}	N_{3t}
λ_{j0}			5.4			9.8	0.0
			(2.8)			(23.3)	(0.0)
$\lambda_{j1} \times 10^{-4}$	130		0.36	229	6.5	5.5	.09
	(30)		(0.06)	(82)	(2.2)	(1.3)	(.01)
$\lambda_{jj} \times 10^{-4}$		5.6	2.1		6.5	2.0	0.7
		(1.5)	(0.6)		(2.2)	(1.3)	(0.2)
$\bar{\gamma}_j \times 10^4$	-0.8	-2.3	-2.5	-0.6	0.2	-3.2	-19.9
	(0.2)	(1.4)	(3.9)	(0.2)	(1.7)	(2.2)	(8.6)
$\delta_j \times 10^4$	6.9	20.2	36.5	5.6	17.8	6.3	103.3
	(0.5)	(1.6)	(2.5)	(0.5)	(1.6)	(6.4)	(7.1)
$\bar{\gamma}_{Vj}$		.0016	.070		.0006	.022	.076
		(.0002)	(.011)		(.0001)	(.003)	(.012)
ρ_j		-1.18	-.05		-1.89	-.02	-.10
		(0.22)	(.01)		(0.40)	(.01)	(.02)
$Corr_j$		-.60	-.92		-.68	-.83	-.76
		(.07)	(.05)		(.09)	(.96)	(.06)
$E[\Delta N^{\text{day}} \mid J]$	5.1	0.22	2.6	5.6	0.16	0.20	1.7
	(1.1)	(0.04)	(0.3)	(1.6)	(0.03)	(0.11)	(0.2)
$E[\Delta N^{\infty} \mid J]$	72	3.1	3.0	112	3.2	0.20	4.9
	(16)	(0.5)	(0.4)	(33)	(0.7)	(0.11)	(1.4)

Table B.V
Variance Factor Loadings

Model and V_i's	$E(V_{it})$	$SD(V_{it})$	Jump variance loading $\lambda_{ji}E(\gamma_j^2)$ on V_{it}				Total variance loading
			$j=0$	1	2	3	
Vjump1a	.0239	.0211		0.22			1.22
V_1	(.0008)	(.0008)		(0.01)			(0.01)
Vjump1b	.0171	.0165	0.50	0.26			1.76
V_1	(.0008)	(.0010)	(0.03)	(0.02)			(0.04)
Vjump2							
V_1	.0116	.0077	0.63	0.23	0.05		1.91
	(.0007)	(.0005)	(0.07)	(0.03)	(0.01)		(0.09)
V_2	.0066	.0431			0.28		1.28
	(.0007)	(.0041)			(0.07)		(0.07)
Vjump3							
V_1	.0085	.0053	0.72	0.21	0.03	0.10	2.05
	(.0008)	(.0005)	(0.13)	(0.04)	(0.05)	(0.02)	(0.17)
V_2	.0049	.0118			0.01		1.01
	(.0006)	(.0009)			(0.02)		(0.02)
V_3	.0051	.0478				0.79	1.79
	(.0013)	(.0115)				(0.14)	(0.14)

Appendix C: Change of Measure

The pricing kernel specification affects three types of parameter values:

1. the risk-neutral jump intensities and average jump sizes
2. the risk-neutral rate of mean reversion of the jump-diffusive spot variance V_{1t}; and
3. the intraperiod conditional mean of futures returns.

For a pricing kernel with log changes of the form

$$d \ln \mathcal{M}_t = \mu_m dt + R\, d \ln F - \sum_i R_{Vi} dV_{it}, \tag{C.1}$$

the transformation from objective to risk-neutral jump intensities is

$$\begin{aligned} \frac{\lambda_{jt}^*}{\lambda_{jt}} &= E_t\left[e^{d \ln \mathcal{M}_t} | dN_{jt} = 1\right] \\ &= \frac{\exp\left(-R\bar{\gamma}_{fj} + \tfrac{1}{2}R^2\delta_{fj}^2\right)}{1 - (R_{Vj} - R\rho_j)\bar{\gamma}_{Vj}} \end{aligned} \tag{C.2}$$

where $\gamma_{fj} \sim N(\bar{\gamma}_{fj}, \delta_{fj}^2)$ and $\gamma_{Vj} \sim Exp(\bar{\gamma}_{Vj})$ are the underlying Gaussian and exponential components of the *j*th log futures jump $\gamma_j = \gamma_{fj} + \rho_j \gamma_{Vj}$.

The risk-neutral distribution for any jump $\tilde{\gamma}$ has a characteristic function

$$E_t^*\left[e^{i\Phi\tilde{\gamma}}\right] = \frac{E_t\left[e^{d \ln \mathcal{M}_t + e^{i\Phi\tilde{\gamma}}} | dN_t = 1\right]}{E_t[e^{d \ln \mathcal{M}_t} | dN_t = 1]} \tag{C.3}$$

The Gaussian shocks γ_{fj} remain Gaussian under this change of measure, with identical variance and shifted mean $\bar{\gamma}_{fj}^* = \bar{\gamma}_{fj} - R\delta_{fj}^2$. The exponential shocks γ_{Vj} remain exponential, with shifted mean

$$\bar{\gamma}_{Vj}^* = \frac{\bar{\gamma}_{Vj}}{1 - (R_{Vj} - R\rho_j)\bar{\gamma}_{Vj}}. \tag{C.4}$$

The overall mean jump in log futures prices becomes $\bar{\gamma}_j^* = \bar{\gamma}_{fj}^* + \rho_j \bar{\gamma}_{Vj}^*$, with associated expected percentage jump $\bar{k}_j^* = \exp(\bar{\gamma}_{fj}^* + \tfrac{1}{2}\delta_{fj}^2)/(1 - \rho_j\, \bar{\gamma}_{Vj}^*) - 1$.

The futures price is a martingale under the risk-neutral measure, with the log futures price evolving as

$$\begin{aligned} df_t &= \sum_{i=1}^{I}\left[-½V_{it}dt + \sqrt{V_{it}}dW_{it}\right] + \sum_{j=1-K}^{J}\left(\gamma_j^* dN_{jt}^* - \lambda_{jt}^*\bar{k}_j^* dt\right) \\ dV_{1t} &= (\alpha - \beta_1^* V_{1t})dt + \sigma\sqrt{V_{1t}}dW_{Vt}^* + \gamma_{V1}^* dN_{1t}^* \\ dV_{it} &= -\beta_i V_{it}dt + \gamma_{Vi}^* dN_{it}^* \text{ for } i > 1, \end{aligned} \tag{C.5}$$

where $\beta_1^* = \beta_1 + R\rho\sigma - R_{V1}\sigma^2$ and N_{jt}^* are Poisson counters with intensity $\lambda_{jt}^* = \lambda_{jt}\left(\frac{\lambda_{jt}^*}{\lambda_{jt}}\right)$.

The instantaneous expected percentage return of the futures price under the objective measure is the conditional equity premium, and takes the form

$$\left(\mu_{0t} + \sum_i \mu_i V_{it}\right)dt = -E_t\left[\left(\frac{dF_t}{F_t}\right)\left(\frac{d\mathcal{M}_t}{\mathcal{M}_t}\right)\right]. \tag{C.6}$$

Because jump intensities are assumed constant within periods, with a linear dependency upon the spot variances at the start of the period, the intra-period parameter values are

$$\begin{aligned} \mu_{0t} &= \sum_j \lambda_{jt}\left(\bar{k}_j - \frac{\lambda_{jt}^*}{\lambda_{jt}}\bar{k}_j^*\right) \\ \mu_1 &= R - R_{V1}\rho\sigma \\ \mu_i &= R \; for \; i > 1 \end{aligned} \tag{C.7}$$

where λ_{jt} is specified in equation (3) and the ratio $\lambda_{jt}^*/\lambda_{jt}$ is a constant given in (C.2).

Table C.I
Objective versus Risk-neutral Parameters from Vjump3 Estimates

rp1: $(R;\ \boldsymbol{R}_V)$ =(2.45; **0**); (β_1, β_1^*) = (54.59, 54.14)
rp2: $(R;\ \boldsymbol{R}_V)$ =(0.075; .001, 10.37, .074); (β_1, β_1^*) = (54.59, 54.58)
rp3: $(R;\ \boldsymbol{R}_V)$ =(300; -933, 2.17, -34.6); (β_1, β_1^*) = (54.59, 31.42)

Jump parameters	Jump *j*			
	0	1	2	3
$\lambda_{jt}^*/\lambda_{jt}$ | rp1	1.0002	0.9996	1.0008	1.0052
$\lambda_{jt}^*/\lambda_{jt}$ | rp2	1.0000	1.0000	1.2916	1.0058
$\lambda_{jt}^*/\lambda_{jt}$ | rp3	1.0328	0.60661	1.1877	1.0640
$\boldsymbol{\bar{\gamma}_{Vj}}$		**0.000637**	**0.0218**	**0.0758**
$\bar{\gamma}_{Vj}^*$ | rp1		0.000638	0.0218	0.0772
$\bar{\gamma}_{Vj}^*$ | rp2		0.000637	0.0281	0.0762
$\bar{\gamma}_{Vj}^*$ | rp3		0.000516	0.0273	0.0591
$\boldsymbol{\bar{k}_j}$	**-0.00608%**	**0.00230%**	**-0.0317%**	**-0.194%**
$\bar{k}_j^*$ | rp1	-0.00616%	0.00153%	-0.0318%	-0.220%
$\bar{k}_j^*$ | rp2	-0.00609%	0.00228%	-0.0469%	-0.199%
$\bar{k}_j^*$ | rp3	-0.01538%	-0.02627%	-0.0487%	-1.384%

Table I
Statistical Properties of the Normalized Returns $z_{t+1} = N^{-1}\left[CDF\left(y_{t+1}|Y_t, \widehat{\Theta}\right)\right]$
for Parameter Estimates $\widehat{\Theta}$ from Various Models

Under correct model specification, the z_{t+1}'s should be independent draws from a Gaussian $N(0,1)$ distribution. Heteroskedasticity-consistent standard errors are in parentheses.

	Vjump1a	**Vjump1b**	**Vjump2**	**Vjump3**
Intradaily and overnight returns (174,854 observations)				
Maximum	6.49	5.46	5.54	4.79
Minimum	-7.38	-5.17	-5.01	-4.41
Mean	.064	.063	.053	0.050
(Std. error)	(.002)	(0.002)	(.002)	(0.002)
Std. deviation	.956	0.970	0.999	1.001
Skewness	.03	0.01	-0.01	-0.02
Excess kurtosis	-.11	-.20	0.02	0.00
Corr(z_{t+1}, z_t)	-.013	-.015	-.012	-.013
(Std. error)	(.003)	(.002)	(.002)	(.002)
Corr$(\|z_{t+1}\|, \|z_t\|)$	.016	.025	.006	-.005
(Std. error)	(.003)	(.003)	(.002)	(.002)
Daily returns (6,558 observations)				
Maximum	4.10	3.99	3.54	3.65
Minimum	-7.39	-7.11	-5.17	-4.16
Mean	0.004	0.013	0.019	0.005
Std. error	0.013	0.013	0.013	0.013
Std. deviation	1.051	1.037	1.028	1.032
Skewness	0.01	0.03	0.00	0.04
Excess kurtosis	0.79	0.53	0.17	0.24
Corr(z_{t+1}, z_t)	-.004	-.006	-.004	-.010
(Std. error)	(.012)	(.012)	(.012)	(.012)
Corr$(\|z_{t+1}\|, \|z_t\|)$	-.070	-.068	-.070	-.067
(Std. error)	(.012)	(.012)	(.012)	(.012)

Table II
Summary Statistics for Daily Realized Volatility Measures

Realized daily volatility is $Rvol_n = \sqrt{\frac{\sum(\Delta \ln F)^2}{252\tau_n}}$, where $252\tau_n$ is the estimated length of the intradaily period in days, with an average value of 0.774 (Vjump1b estimates). ARMA models are estimated in RATS, using the Bayes information criterion for model selection.

	$\boldsymbol{Rvol_n^2}$	$\boldsymbol{Rvol_n}$	$\boldsymbol{\ln(Rvol_n)}$
Maximum	0.027530	26.93%	-1.312
Minimum	0.000003	0.17%	-6.380
Mean	0.000130	0.91%	-4.825
(Std. error)	(0.000012)	(0.01%)	(0.006)
Median	0.000062	0.79%	-4.847
Std. deviation	0.000982	0.68%	0.477
Skewness	63.4	12.5	0.63
Excess kurtosis	4553	367	1.83
ARMA model	ARMA(3,1)	ARMA(3,1)	ARMA(3,2)

Major $Rvol_n$ outliers: 26.9% (10/20/1987), 14.8% (10/19/1987), 11.4% (10/22/1987), and 8.7% (10/10/2008).

Table III
Forecasts of Average Daily Realized Variances over 1983-2016

Sample moments for realized variances are in squared percentages. An average intradaily realized variance of 1.31 over 1983 to 2008 corresponds to a 1.14% realized volatility, scaled as in Table II to a daily horizon. VIX-based forecasts of average realized variances over 21 business days use the regression

$$252\overline{RV}_{t+1\to t+21} = \underset{(0.49)}{-0.08} \underset{(0.77)}{-0.19}\, VIX_t + \underset{(0.30)}{0.89}\, VIX_t^2$$

on daily data over 1990-2008. Standard errors are in parentheses, corrected for heteroscedasticity and for serial correlation from overlapping forecasts.

	Intradaily realized variance (scaled)			Intradaily/overnight
	1-day	5-day	21-day	21-day RV
1983-2008 (in sample): Avg(RV) = 1.31 intradaily, 1.43 intradaily & overnight				
SD(RV):	9.83	6.06	3.62	4.73
R^2				
ARMA(3,1)	0.132	0.087	0.063	
Vjump1b	0.139	0.128	0.094	0.101
Vjump2	0.161	0.099	0.099	0.120
Vjump3	0.270	0.174	0.132	0.137
1990-2008 (in sample): Avg(RV) = 1.18 intradaily, 1.26 intradaily/overnight				
SD(RV):	2.69	2.23	1.97	2.17
R^2				
ARMA(3,1)	0.440	0.421	0.288	
Vjump1b	0.535	0.585	0.350	0.327
Vjump2	0.517	0.521	0.366	0.342
Vjump3	0.503	0.610	0.440	0.419
VIX-based				0.537
2009-16 (out of sample): Avg(RV) = 0.94 intradaily, 1.17 intradaily/overnight				
SD(RV):	1.90	1.37	1.09	1.32
R^2				
ARMA(3,1)	0.280	0.345	0.317	
Vjump1b	0.351	0.445	0.319	0.333
Vjump2	0.360	0.501	0.436	0.454
Vjump3	0.314	0.447	0.475	0.537
VIX-based				0.569

Table IV

Summary Statistics for the Residuals $z_{n+1} = N^{-1}\left[CDF^{QV}\left(RV_{n+1}\middle|Y_{n,M_n}, \widehat{\Theta}\right)\right]$ over 1983-2008, on Actual and Simulated data

Normalized residuals should be i.i.d. standard Gaussian conditional upon correct specification. Simulated data are from 100 runs of 6557 days each, using model-specific parameter estimates and time gaps. The *t*-statistics for compatibility between actual and simulated moments are $\left[M^{act} - Avg\left(M^{sim}\right)\right] / \left[SD\left(M^{sim}\right)\sqrt{1.01}\right]$.

	Actual	Simulated data		
Statistic	**Data**	**Average**	**Std. deviation**	***t*-statistic**
Vjump1b				
Maximum	>7[a]	3.80	0.34	9.41
Minimum	-7.55	-4.52	0.42	-7.17
Mean	-0.191	-0.106	0.012	-7.27
Median	-0.155	-0.093	0.017	-3.59
SD	**1.265**	**1.158**	**0.011**	**9.99**
Skewness	-.32	-.12	0.03	-8.17
Excess kurtosis	0.55	-.28	0.05	16.40
Vjump2				
Maximum	6.46	3.80	0.31	8.52
Minimum	-5.50	-5.13	0.52	-0.71
Mean	-0.225	-0.163	0.014	-4.35
Median	-0.121	-0.096	0.022	-1.16
SD	**1.250**	**1.211**	**0.009**	**4.10**
Skewness	-0.40	-0.28	0.03	-3.50
Excess kurtosis	0.16	-0.13	0.06	4.41
Vjump3				
Maximum	5.88	3.80	0.34	6.04
Minimum	-5.62	-5.01	0.40	-1.53
Mean	-0.190	-0.156	0.012	-2.77
Median	-0.119	-0.112	0.017	-0.39
SD	**1.245**	**1.215**	**0.011**	**2.88**
Skewness	-0.33	-0.20	0.03	-3.78
Excess kurtosis	0.20	-0.10	0.07	4.53

[a]The normalized residual observed on October 20, 1987 could not be computed for the Vjump1b model, but is in excess of 7. The summary statistics use a value of 7 for that observation.

Table V
Option and Time Series Fits from Various Specifications of Risk Premia

rp1: $(R;\ \boldsymbol{R}_V) = (2.45;\ \mathbf{0})$; rp2: $(R;\ \boldsymbol{R}_V) > 0$; rp3: unconstrained $(R;\ \boldsymbol{R}_V)$.

IV-RMSE is the overall fit to all short-maturity options' implicit volatilities over 1990-2016. $\Delta \ln L \mid \{\hat{g}_{t|t}\}$ is the change in log likelihoods of intradaily and overnight returns over 1983-2016 from the resulting changes in the conditional equity premium, with filtered $\hat{g}_{t|t}$ unchanged. $\widehat{IV}^{atm}$ is the predicted at-the-money implicit volatility. $\widehat{SKEW} = \widehat{IV}^{call} - \widehat{IV}^{put}$ is the predicted slope of the volatility smirk, using calls and puts that are one standard deviation out-of-the-money.

	Overall *IV-RMSE*, in %				Time series: $\Delta \ln L \mid \{\hat{g}_{t|t}\}$		
	rp1	**rp2**	**rp3**		**rp1**	**rp2**	**rp3**
Vjump1b	4.41	4.37	4.32		5.49	1.58	-1,484
Vjump2	4.49	4.00	3.93		5.50	6.76	-26,533
Vjump3	4.00	3.79	3.63		-10.41	-12.00	-7,814

	$Avg(\widehat{IV}^{atm})$			**data**	$RMSE(\widehat{IV}^{atm})$		
Vjump1b	17.15	17.48	17.38	**17.06**	4.05	4.03	4.02
Vjump2	15.86	16.75	16.68	**17.06**	4.09	3.75	3.81
Vjump3	15.52	16.78	16.83	**17.06**	3.73	3.29	3.28

	$Avg(\widehat{SKEW})$			**data**	$RMSE(\widehat{SKEW})$		
Vjump1b	-1.86	-1.91	-2.03	**-3.97**	2.72	2.72	2.61
Vjump2	-2.11	-2.27	-2.60	**-3.97**	2.37	2.31	2.06
Vjump3	-2.16	-1.90	-2.37	**-3.97**	2.24	2.54	2.18

Table VI
Average $\widehat{SKEW}$ by Maturity (in Business Days)

Average estimated $\widehat{SKEW} = \widehat{IV}^{call} - \widehat{IV}^{put}$ and corresponding observed values for the specified maturities are based upon 311 - 316 monthly observations over 1990-2016.

	Vjump1b			Vjump2			Vjump3			
	rp1	**rp2**	**rp3**	**rp1**	**rp2**	**rp3**	**rp1**	**rp2**	**rp3**	**data**
1-day	-1.25	-1.30	-1.34	-1.32	-1.41	-1.72	-1.22	-1.32	-1.76	**-2.46**
5-day	-1.95	-2.01	-2.11	-2.08	-2.26	-2.59	-1.92	-1.81	-2.31	**-3.46**
18-day	-1.83	-1.87	-2.01	-2.19	-2.33	-2.66	-2.45	-2.02	-2.45	**-4.70**

Figure 1. Overnight (ON) and intradaily (ID) return horizons, relative to Wednesday (Tuesday close → Wednesday close). Overnight returns for Monday (Friday close → Monday open) and for Tuesday through Friday include the first 15 minutes of the opening day, as do overnight returns spanning 2-day holidays and 4- or 5-day holiday weekends.

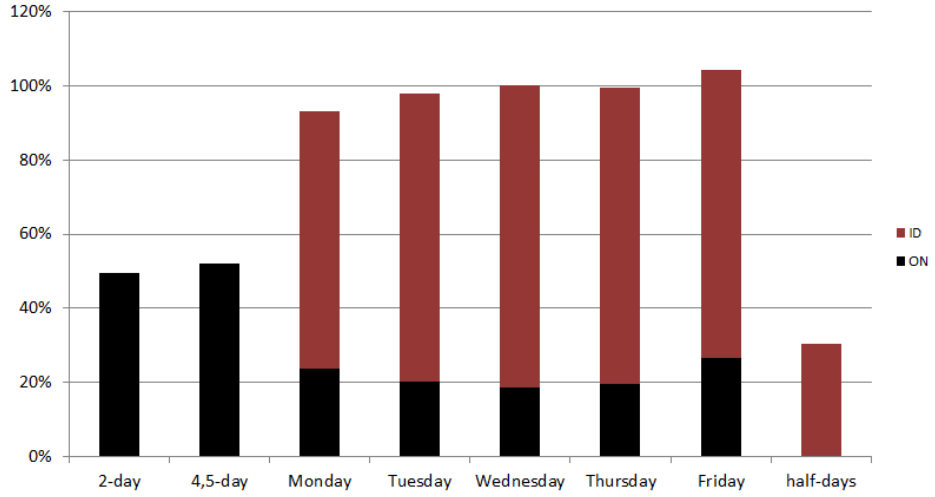

Figure 2. Estimated intradaily 15-minute horizons and quadratic variation over 1985 to 2008, as percentages of the intradaily totals. The shaded areas indicate the period-specific estimated components of quadratic variation from the Vjump1b model. The black rectangles are period-specific realized variances as percentages of total intradaily estimated quadratic variation.

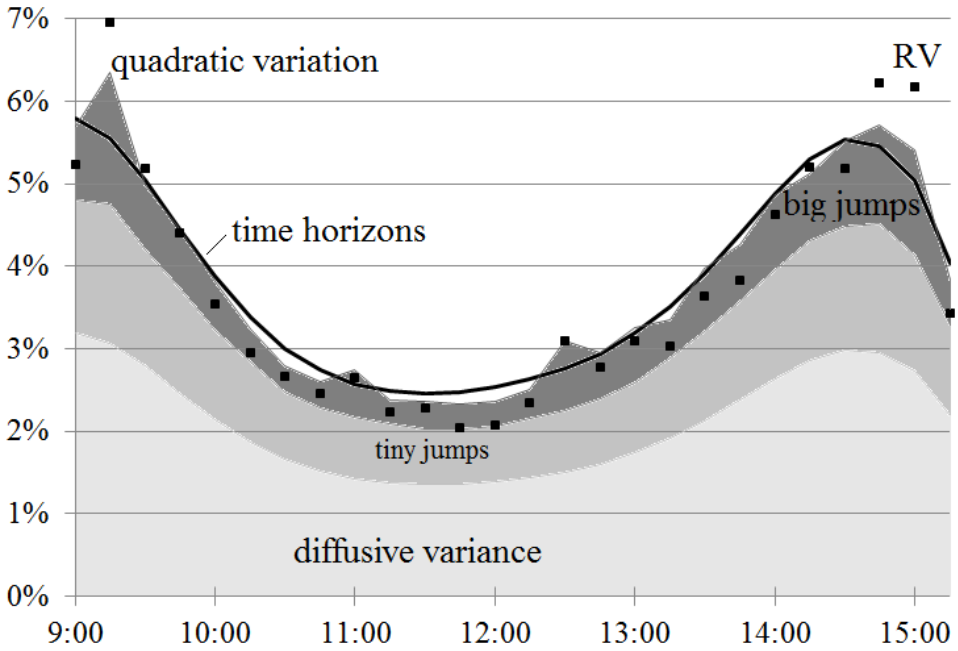

Figure 3. Cumulative log likelihood improvements relative to the 1-factor SVJ1 model, and impact of eliminating self-exciting jumps in the Vjump2 and Vjump3 models.

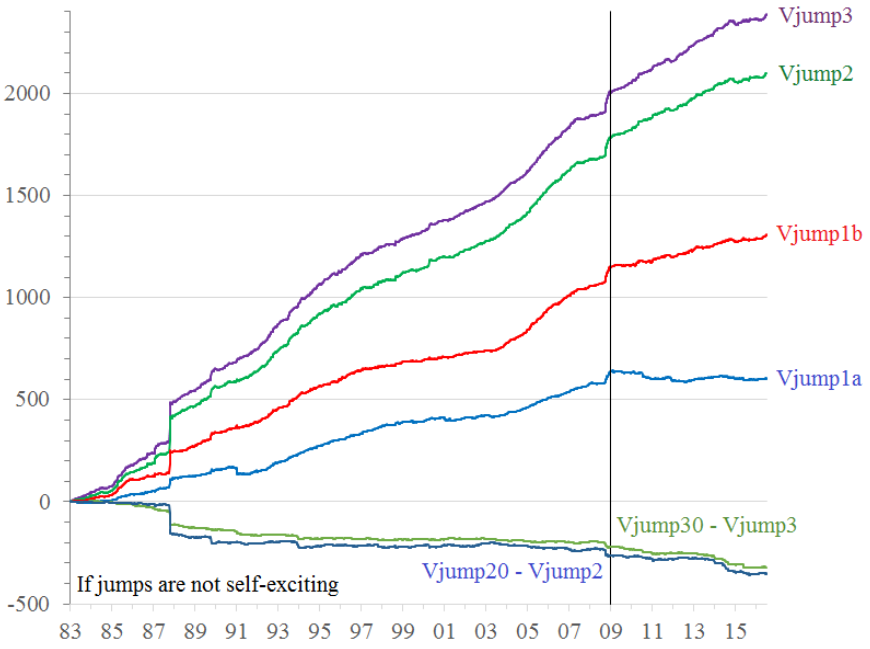

Figure 4. Components of annualized conditional volatility, and daily estimated number of jumps, 1983 to 2016. Total end-of-day variance estimates V_{it}^{tot} from the 3-factor variance model Vjump3 include the contributions to both diffusion risk and jump risk.

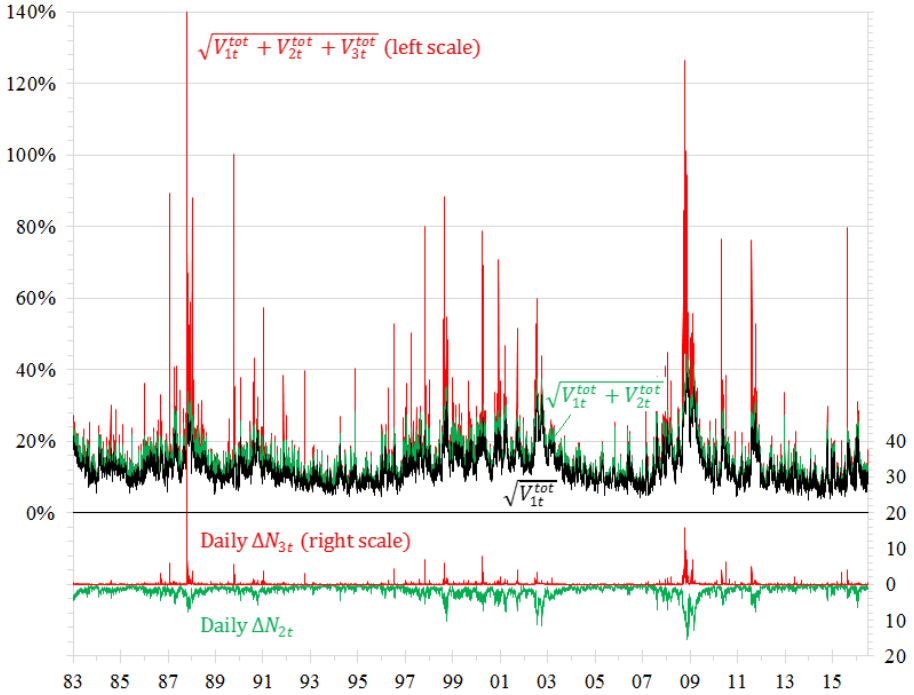

Figure 5. Annualized intradaily conditional volatility factors over October 12-30, 1987 (100% annualized = 1.1% per quarter-hour). The December 1987 S&P 500 futures price (+) is on the right scale.

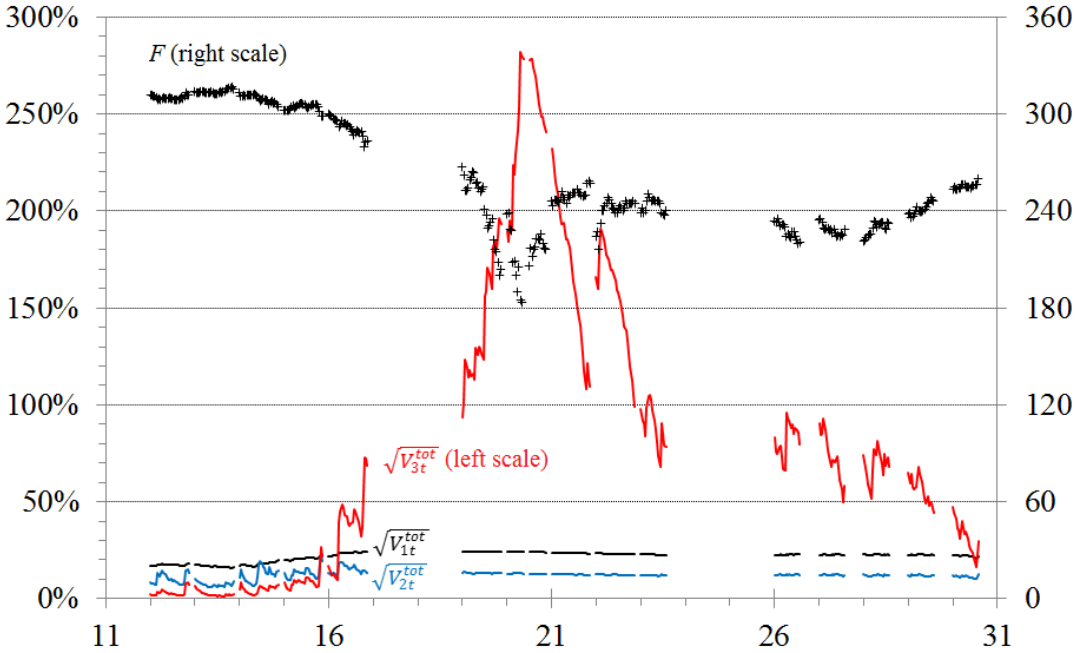

Figure 6. Annualized intradaily conditional volatility factors over September and October, 2008 (100% annualized = 1.1% per quarter-hour). September and December 2008 S&P 500 futures prices (+) are on the right scale.

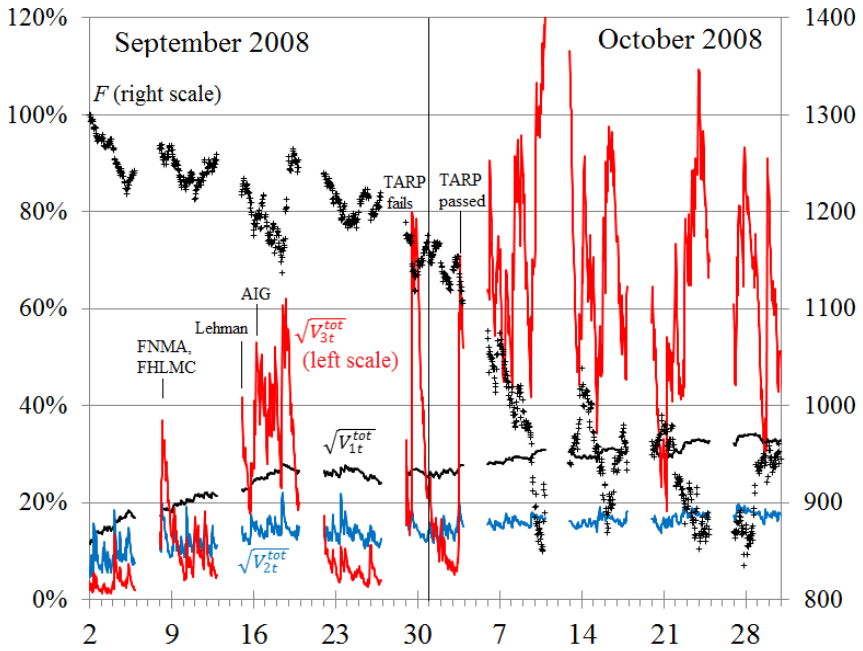

Figure 7. Normal probability plots for various models. The first column shows the ordered normalized residual values $z_{t+1} = N^{-1}\left[CDF\left(y_{t+1}\middle|\boldsymbol{Y}_t, \widehat{\Theta}\right)\right]$ (+ symbols on the vertical axis), compared with the models' predicted values (red diagonal line) over 1983 to 2008. The second column is the same for daily returns, using data $\boldsymbol{Y}_t$ up through the end of the preceding day. Grey areas indicate 95% confidence intervals from 100 simulated paths.

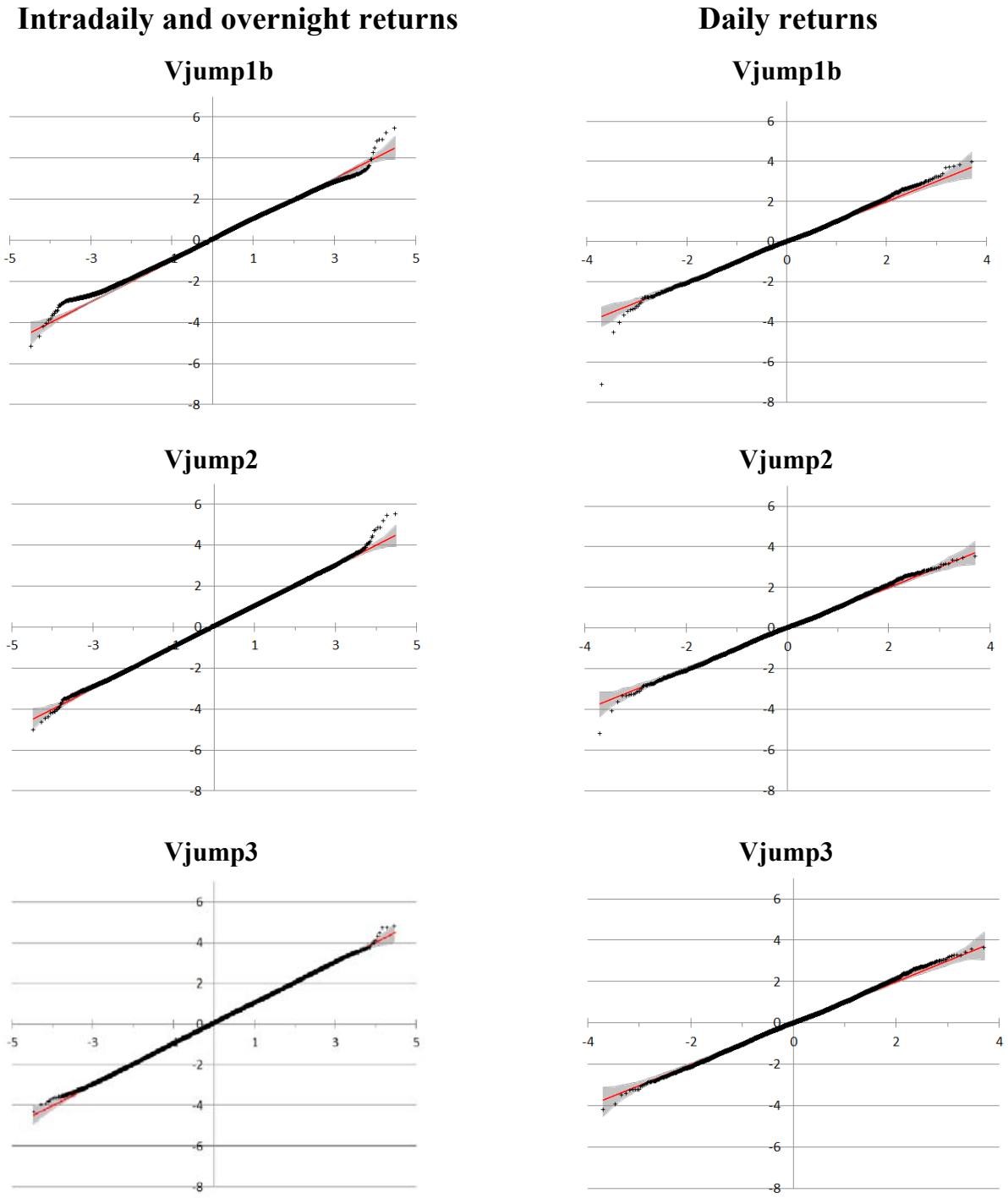

Figure 8. Daily realized variance (regular scale) and volatility (log scale).

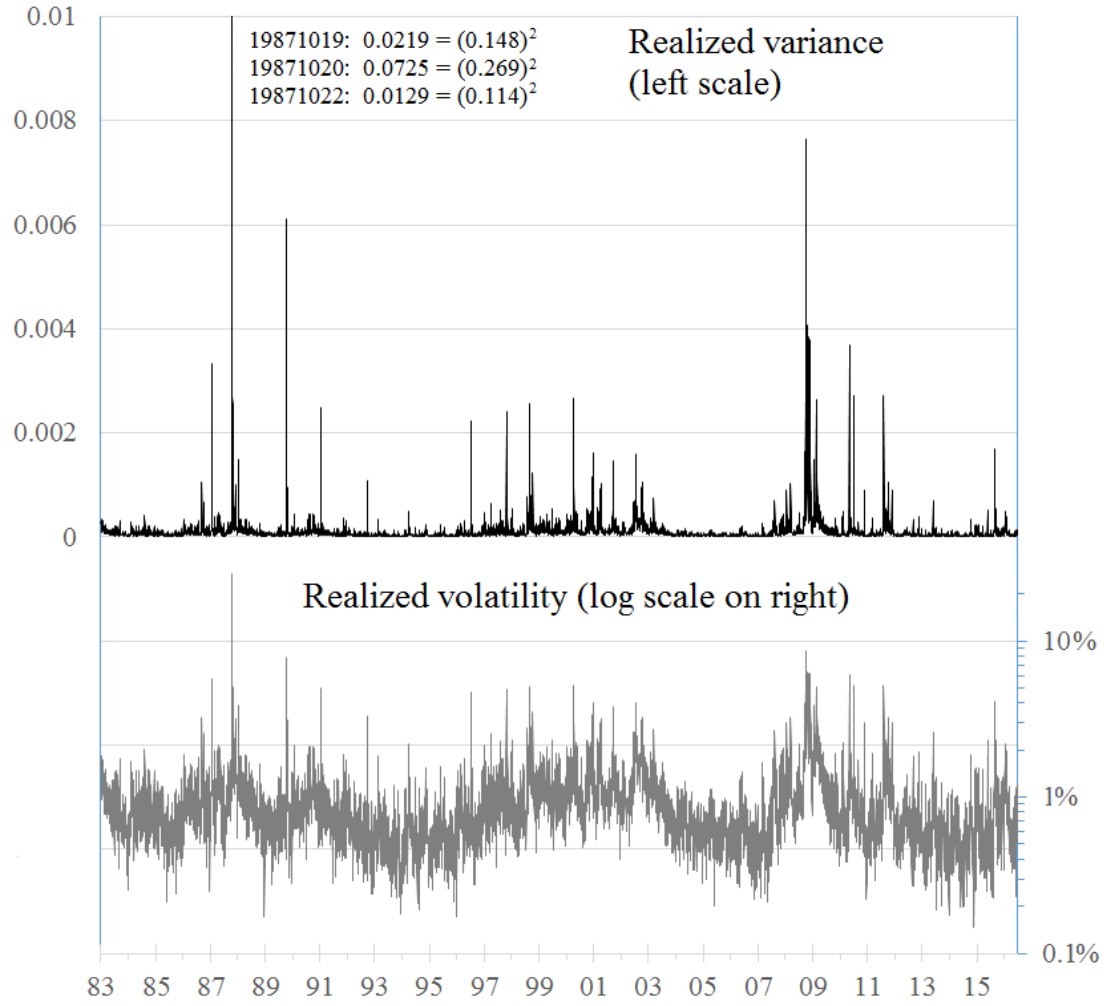

Figure 9. Normal probability plots for realized variance. These compare the ordered normalized residual values $z_{n+1} = N^{-1}\left[CDF^{QV}\left(RV_{n+1}\middle|\boldsymbol{Y}_{n,M_n}, \widehat{\Theta}\right)\right]$ (+ symbols on the vertical axis) with predicted values (green dotted lines) based upon quadratic variation's conditional CDFs, and with average values (red solid lines) from 100 runs of simulated data. The grey shaded areas are 95% confidence intervals for the deviation between observed data and average simulated values.

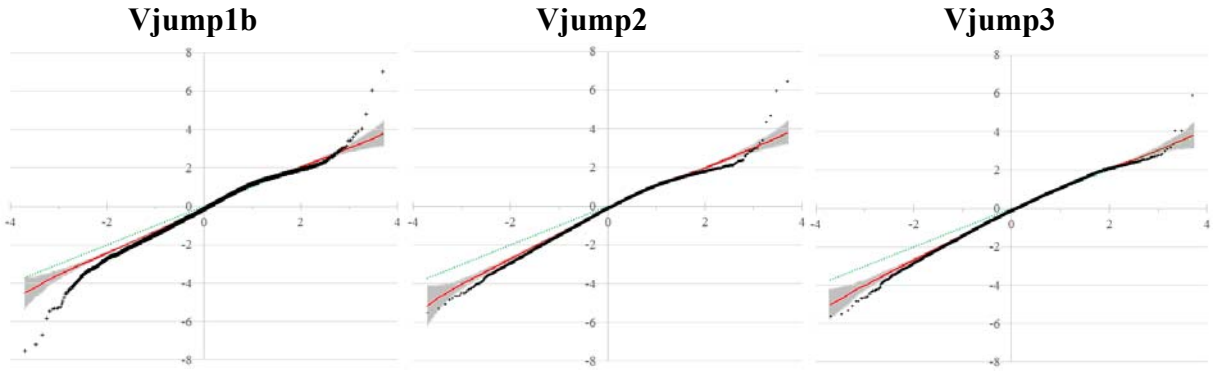

Figure 10. Observed and estimated at-the-money implicit volatilities IV^{atm}, and divergences $SKEW = IV^{call} - IV^{put}$ for calls and puts one standard deviation out-of-the-money. Option maturities are the shortest available with at least one day to maturity.